Agricultural and Forest Meteorology 260–261 (2018) 17–30

Contents lists available at ScienceDirect

Agricultural and Forest Meteorology

journal homepage: www.elsevier.com/locate/agrformet

Tropical Montane Cloud Forests in the Orinoco River basin: Inferring fog interception from through-fall dynamics

Beatriz H. Ramírez[a,b,*], Lieke A. Melsen[c], Laurens Ganzeveld[d], Rik Leemans[e], Adriaan J. Teuling[c]

[a] Water Systems and Global Change Group, Wageningen University & Research, Netherlands
[b] Centro de Estudios Ambientales de la Orinoquia, Asociación de Becarios de Casanare, Colombia
[c] Hydrology and Quantitative Water Management Group, Wageningen University & Research, Netherlands
[d] Meteorology and Air Quality Group, Wageningen University & Research, Netherlands
[e] Environmental Systems Analysis Group, Wageningen University & Research, Netherlands

ARTICLE INFO

Keywords:
Interception
Rutter model
Forest succession
Hydrology
Eastern Andes

ABSTRACT

The interaction between vegetation and the atmosphere is highly complex in fog affected ecosystems like Tropical Montane Cloud Forests (TMCFs). Despite acknowledging fog effects on the canopy's water balance, quantifying their influence remains challenging. While the reduction in potential evaporation that is caused by fog presence, is largely independent of land cover, fog interception itself strongly depends on the land-cover's vegetation characteristics. A better understanding of how these two fog related processes affect the water balance is highly relevant under current land-use and climate-change pressures. In this study we evaluate the different fog effects on TMCFs' canopy interception combining model simulations and high temporal resolution (10 min) observations that were collected in different TMCF regeneration stages: early succession, secondary and old-growth TMCFs. We also analyse the difficulties in closing catchment water balances caused by limitations on the interpretation of throughfall data to properly represent these fog effects.

Results show that different fog frequencies along elevation affect potential evaporation. The higher elevation old-growth TMCFs have a lower simulated evaporation and a lower dry canopy frequency than the low elevation secondary and early succession forests. Furthermore, we show that fog water inputs during fog-only events, even though higher at the higher elevation, are irrelevant as water inputs (from 0.8% to 1.6% of measured rainfall), but fog's contribution to through-fall during foggy rainfall events can be more relevant (from 5.8%–12.8% of measured rainfall). Additional to the fog trends along the elevation, we also uncover variable fog-vegetation interactions controlled by differences in canopy water storages as a function of forest cover. Each evaluated process has associated uncertainties, which together cumulatively explain why closing a water budget in TMCF catchments is limited by data collection methods that probably do not capture all relevant fog effects. In addition, this study also indicates that the temporal resolution of measured rainfall and through-fall and compensating effects of canopy parameters that are estimated by the commonly used Rutter canopy-rainfall interception model, pose an additional challenge to understand and quantify fog effects in the water budgets of TMCFs.

1. Introduction

Understanding the consequences of land-use and climate changes for hydrologic processes is a major scientific challenge (DeFries and Eshleman, 2004; Hooke et al., 2012; Wagener et al., 2010). The implications of these changes on the water cycle, and ultimately water availability at variable spatial and temporal scales, are subject to considerable debate and research (e.g. Ellison et al., 2017; Balthazar et al., 2015; Bonell, 2010; Ellison et al., 2012). Canopy interception is a relevant water-balance component that is affected by land-use change (Piao et al., 2007), and also potentially by climate change (Wallace and McJannet, 2012, 2013). Interception can strongly affect water yields (Van Dijk and Peña-Arancibia, 2012) and also precipitation through intensified land-atmosphere interactions (Guillod et al., 2014). Deforestation and subsequent forest recovery induce changes in canopy characteristics that determine the canopy's water storage and drainage rates (Holwerda et al., 2010; Ponette-González et al., 2010; Pryet et al., 2012), while changes in rainfall (P) and potential evaporation (PE) affect the input and losses of water from the canopy (Crockford and Richardson, 2000). The interaction between the vegetation and the

* Corresponding author at: Water Systems and Global Change Group, Wageningen University & Research, P.O. Box 47, 6700 AA, Wageningen, Netherlands.
E-mail address: beatriz.ramirezcorreal@wur.nl (B.H. Ramírez).

https://doi.org/10.1016/j.agrformet.2018.05.016
Received 7 September 2017; Received in revised form 11 May 2018; Accepted 21 May 2018
Available online 05 June 2018

atmosphere is even more complex in fog affected ecosystems like Tropical Montane Cloud Forests (TMCFs; Chu et al., 2014; Dietz et al., 2007).

Fog persistence plays a key role in modulating TMCFs' unique hydrology (Grubb, 1977). Fog affects evapotranspiration and thus plant-water relations by reducing incoming solar radiation, increasing leaf wetness frequency and decreasing atmospheric vapour pressure deficit (Letts and Mulligan, 2005; Reinhardt and Smith, 2008; Eller et al., 2015). Reduced transpiration results in less water uptake from the soils and reduced canopy evaporation can increase through-fall, both sustaining higher moisture conditions in the system. Furthermore, fog interception by the canopy provides an additional water input to rainfall (Zadroga, 1981) and potentially induce foliar water uptake (Eller et al., 2015; Goldsmith et al., 2013). The previously described fog effects on TMCFs' hydrology suggest that TMCFs play a key role in regulating streamflows (e.g. Roa-García et al., 2011; Ramírez et al., 2017b). Despite their hydrological relevance, TMCFs are vulnerable to land-use and climate changes (Scatena et al., 2011). On the one hand, land-use change poses a major threat as more than half of TMCFs world-wide were converted to other land use types by the year 2000 (Mulligan, 2011). On the other hand, climate change can alter the elevation at which fog occurs exposing TMCFs to drier atmospheric conditions (Still et al., 1999).

Although the effect of fog on the canopy water balance is acknowledged, quantifying its influence remains challenging (Frumau et al., 2011). Indirect approaches, such as identifying thresholds of meteorological variables to infer fog's contribution to through-fall has been possible for drier environments with a clear meteorological signature (e.g. Marzol, 2008) but not so for extremely wet environments where fog does not have a clear meteorological signature (e.g. Brauman et al., 2010). Also, several direct measurement methods have been employed to quantify fog's liquid water content including passive or active fog collectors, fog detectors and fog/cloud droplet spectrometers. However, they all have their caveats concerning, for example, the discrimination between fog and wind-driven rainfall, minimum water content thresholds and fog droplet size distribution. These caveats are discussed in detail by Bruijnzeel et al. (2006). Additionally, these methods are point measurements and this limits their spatial representativeness. Furthermore, quantifying fog's liquid water content alone is insufficient to determine the canopy's fog interception rates. The fog-vegetation interaction also depends on wind speed and vegetation characteristics, like canopy roughness and canopy leaf area, leaf surface texture (e.g. hydrophilic hairs or hydrophobic waxes), leaf inclination and exposition to wind direction (Crockford and Richardson, 2000; Herwitz, 1985). To our knowledge only a few studies focusing on relatively few species (< 13 spp) have considered most of the above mentioned canopy characteristics (e.g. Holder and Gibbes, 2017; Garcia-Estringana et al., 2010). The required information on canopy characteristics is already overwhelming, but determining all these features is impossible in montane (> 1000 m asl) tropical forest contexts, where plant diversity can reach up to 100 spp per 0.1 ha (Gentry, 1988). A more practical approach is to evaluate the fog/vegetation interaction at the catchment scale with effective parameters that represent the high spatial variability within the canopy.

A common approach to study fog and canopy interactions is to compare interception and through-fall (hereafter TF) between areas or seasons with contrasting fog influence, and/or between different land-cover types (e.g. Brauman et al., 2010; Giambelluca et al., 2011; Ponette-González et al., 2010; Pryet et al., 2012). To quantify interception, precipitation above and below the canopy (i.e. TF) is measured. These comparisons allow to quantify the additional water input by fog reflected in additional TF. However, given the high temporal variability of fog occurrence at daily or shorter timescales, this quantification is likely sensitive to the temporal resolution of the measurements, which varies considerably throughout the literature (e.g. weekly: Gómez-Peralta et al., 2008; Fleischbein et al., 2005; Wullaert et al., 2009; daily: Hölscher et al., 2004; and 10 min: Holwerda et al., 2010). Furthermore, the rainfall-through-fall approach does not provide information on the relative contribution of the multiple processes affected by fog that control the canopy water balance. For example, evaporation varies between very high levels for clear sky conditions to very low levels under cloud/fog influence (Hidalgo et al., 2005), leading to contrasting canopy drying times. At the same time, the canopy water storage can also be filled by fog interception. These interactions between fog and the canopy water balance remain difficult to quantify.

Fog incidence depends mostly on upwind and local hydrometeorological conditions. Thus, the expected climate changes regarding the length and severity of dry and wet seasons for the region (Magrin et al., 2014) can potentially alter fog formation. In contrast, fog interception by the vegetation depends on vegetation characteristics associated with land cover (e.g. Holwerda et al., 2010). Therefore, under current land-use and climate change pressures it is highly relevant to better understand how the two processes of reduced evaporation and fog interception affect the water balance of ecosystems, such as TMCFs.

Canopy interception models allow to integrate the through-fall/rainfall (TF/P) processes by considering rainfall, evaporation, drainage outputs and canopy characteristics. Muzylo et al. (2009) review canopy interception models and their use worldwide. The two most commonly used interception models are the Rutter model (Rutter et al., 1971, 1975; Rutter and Morton, 1977) and the Gash model (Gash, 1979). The Rutter model is a process-based continuous water-balance model with two empirical drainage parameters. The Gash model is the analytical version of the Rutter model with reduced data requirements and it is thus more widely used (Muzylo et al., 2009). The Gash model partitions individual rainfall events into three stages: wetting up, saturation and evaporation after rainfall ceases, but it requires the discretization of rainfall events assuming to have a dry canopy preceding each event. The validity of this assumption is questionable in fog affected forests where fog is not detected by rain gauges. The continuous Rutter model does not rely on the assumption of a dry canopy. Furthermore, the continuous water-balance calculation provides insights in the water stored in the canopy in-between rainfall events and this allows to determine the dry/wet canopy frequency. Hence, the Rutter model is best suited to integrate meteorological data with TF data to understand the fog effect on the canopy water balance in TMCFs.

In this study, we aim to estimate the multiple fog effects on the canopy water budget in three successional TMCF stages. Our analyses are based on TF and meteorological data coupled with canopy interception modelling. To achieve our aim we will address the following research questions (RQs; see also Fig. 1):

RQ1. How does the temporal resolution of measured rainfall and through-fall affect the estimates of additional water inputs by fog?

RQ2. What is the potential effect of different fog intensities on evaporation and how does this affect the partitioning of rainfall between through-fall and evaporation for the three main forest covers in our study area?

RQ3. How (seasonally) relevant are the fog water inputs during fog-only events in the three main forest covers in our study area?

RQ4. What is the fog effect on through-fall during rainfall in the three main forest covers?

To answer the research questions we monitored at a 10 min time resolution for more than a year, three neighbouring catchments located within the Colombian Orinoco River basin with different land covers: old-growth TMCF (OGF), secondary (SECF) and early successional stages (EARF) and grasslands. Previous studies on these catchments have shown that there are missing sources of water to close the water budgets (Ramírez et al., 2017a). A positive correlation between fog/

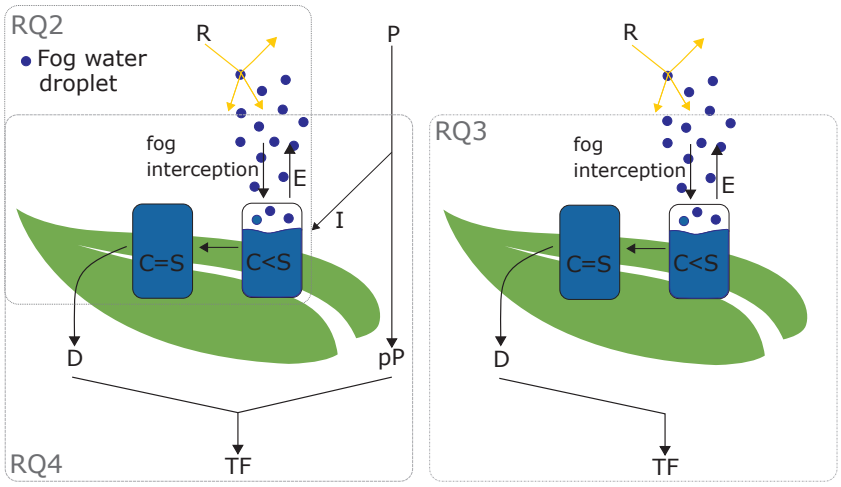

Fig. 1. Conceptualization of processes related to canopy interception and the research questions addressed in this study (RQ2 to RQ4). The conceptualization represents canopy interception (I) of rainfall (P), the proportion of rainfall that passes through the canopy gaps (pP) and the effects of fog in partially reflecting and scattering radiation (R) and reducing evaporation (E; RQ2), filling the canopy water storage (water stored -C in relation to the canopy water storage -S) and draining (D) during fog only events (RQ3), and enhancing through-fall (TF) during events with both fog and rainfall (P; RQ4).

clouds and elevation suggests that fog interception at the higher elevations could contribute to streamflows (Ramírez et al., 2017a). Another contribution could come from the soil water storage. So far, we have also identified an important role in water storage and release from the soil organic layer in TMCFs (Ramírez et al., 2017b). However, until this study, neither differences in Potential Evaporation (PE) nor fog inputs along elevations and/or between seasons for this specific area had been assessed.

2. Materials and methods

2.1. Study area

We collected data from August 1st 2014 to June 12th 2016 in three adjacent headwater catchments that are located on the eastern slope of the eastern Andean Cordillera (72.900 E-5.243 N; Fig. 2), in the municipality of Chámeza (Casanare, Colombia). The eastern Andes are dominated by young mountains with steep slopes and sharp crests (Stallard et al., 1991). From a biogeographical perspective this study area belongs to the Andean region, while hydrologically, it is part of the Orinoco River basin highlands. The catchments have a total area of 10.2 km^2, cover an elevation range between 1550 and 2490 m asl and are located windward. Climate data from April 2014 to April 2016 showed a mean daily temperature of 16.5 °C and 14.5 °C at 1819 m asl and at 2148 m asl, respectively. Mean annual rainfall ranged between 4283 mm at 1550 m asl and 4966 mm at 2148 m asl. Its mono-modal rainfall regime has a dry season from December to March during which less than 16% of annual rainfall occurs (Ramírez et al., 2017a). Mean observed daily wind speed and maximum hourly values were higher at 1819 m asl (1.5 m s^{-1} ± 0.4 m s^{-1}, max = 7.3 m s^{-1}) than at 2148 m asl (0.7 ± 0.2 m s^{-1}, max = 5.5 m s^{-1}; Ramírez et al., 2017a). The dominant daytime winds were easterlies (68° to 113°), whilst night time winds were predominantly westerlies (270° to 293°; Ramírez et al., 2017a). Previous fog event analyses revealed a positive relation between fog occurrence and elevation, and less fog events during the dry season compared to the wet season. Diurnal fog patterns in both seasons showed an increase of fog events during the afternoon until 20 h (Ramírez et al., 2017a). The study area's current land cover consists of evergreen old-growth TMCF (OGF), secondary TMCF (> 10 yr; SECF), young secondary forest (< 10 yr; EARF), grasslands and small-scale agricultural areas.

In our analyses, we will assess canopy interception on different forest covers. OGFs are mainly found at the higher elevations on the steeper slopes in contrast to SECFs and EARFs, and according to local inhabitants, they have never been cleared. However, OGFs are occasionally subjected to selective logging. OGFs are characterized by emergent trees (> 30 m) and a lower more homogeneous canopy (i.e. 15–20 m) with a high epiphyte cover (bromeliads and mosses) on tree trunks and branches, and a relatively open understorey. *Cyathea sp*, *Alchornea sp*, *Hedyosmum sp* and *Weinmannia sp* were identified as dominant tree species according to a preliminary inventory (Stevenson and Casas, 2008). Vegetation studies in OGFs located in the Colombian eastern Andes, 200 km southwest of our study area, reported 37 spp of trees (> 10 cm DBH) and between 10–13 spp of vascular and non-vascular epiphytes in a total of 0.35 ha (1120–2500 m asl; Cantillo and Rangel, 2008). Further south, in the National Natural Park Cueva de los Guácharos (1765–2204 m asl), Prada and Stevenson (2016) recorded between 55–86 plant species per 0.1 ha (> 2.5 cm DBH).

SECFs are found mainly on the edges of OGFs. They were OGFs before being cleared through slash-and-burn for agriculture or grasslands. These areas were afterwards abandoned and allowed to regenerate. SECFs have tall trees (up to 20 m) but not emergent ones as in OGFs and even though they also present a high epiphyte cover, it is comparatively lower than in OGF. SECF's understorey can vary from being very open to very close due to the presence of broad banana-leafed Zingiberales clusters. EARFs are in the earliest forest succession stage. They were previously grasslands or croplands but they were abandoned (< 10 years) as part of the local rotational agricultural practices. Trees can reach up to 10 m of height and most of them are early succession taxa such as *Cecropia, Siparuna* and *Vismia*. Below them, there is a dense canopy of other woody species shorter than 8 m and an even denser shrubby understorey with spiny ferns and various Zingiberales species. Epiphyte cover is less developed than in the other two forest types, mainly due to less trunk and branch surface area given the fairly young stand age.

2.2. Data collection

2.2.1. Rainfall data

We installed two Decagon ECRN-100 rainfall gauges at 2 m above the ground. Data from each gauge were recorded at 10 min intervals on a Decagon EM50 data logger. One rainfall gauge was located at 2148 m asl on a large clearing (> 900 m^2) inside the forest (RS_{2148}; Fig. 2). The other was located on a grassland at 1819 m asl (RS_{1819}). We applied the Førland and Hanssen-Bauer (1996) wind correction model to rainfall data. Wind data were obtained from the closest weather station (see section 2.2.2).

2.2.2. Meteorology and estimation of potential evapotranspiration

Meteorological data were collected with two Davis Vantage Pro2-plus automated weather stations (AWS; Fig. 1). One AWS was located at a lower elevation (1819 m asl) on a grassland site at 2 m from the ground (72.907 E, 5.231 N; AWS_{1819}). The second AWS was located at higher elevation (2148 m asl) at 17 m above the ground in a scaffolding

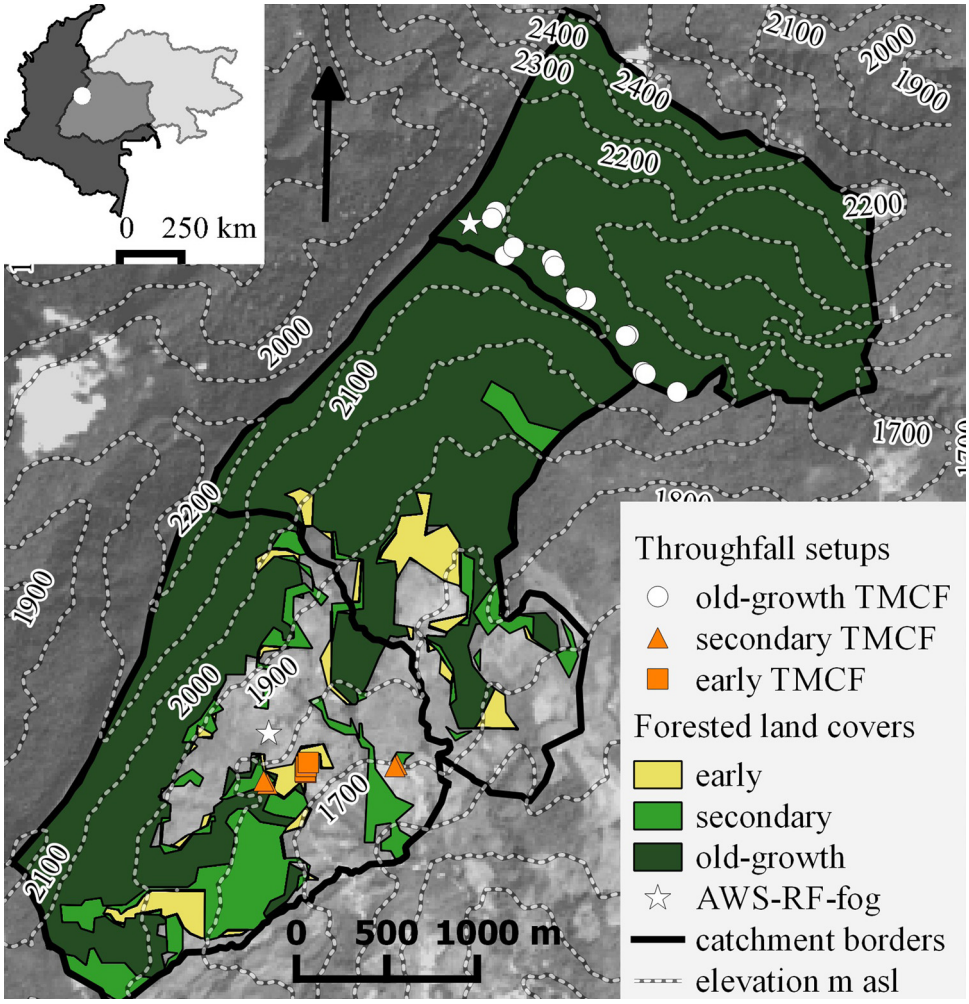

Fig. 2. Map of study area and experimental setup. The inset map shows the Orinoco river basin (light grey) and its overlap with Colombia (dark grey). The white dot represents the study area, enlarged on the main map. This map shows: 1) Land cover classification: old-growth TMCFs, secondary TMCFs, and early TMCFs. 2) Location of the through-fall setups in each land cover type. 3) Location of the AWSs, rainfall and fog gauges. 4) Elevation contours and 5) Catchment borders. The background image is the band 8 (15 m resolution) of a Landsat 8 image taken on December 25th, 2013.

tower surrounded by a forest canopy of c.16 m. Therefore, the meteorological station was 1 m above the surrounding canopy (72.897 E, 5.257 N; AWS_{2148}). Both stations recorded the following mean daily data on a Weatherlink datalogger at 10 min intervals: shortwave incoming radiation (Vantage-Pro2 6450 Solar pyranometer); relative humidity (passively shielded film capacitor element), air temperature (passively shielded PN Junction Silicon diode), wind speed (large cup anemometer); and barometric pressure.

To estimate the Potential Evaporation (PE) at each AWS elevation we used the Penman–Monteith model (Monteith, 1965) assuming a single-layered canopy with zero stomatal resistance. Setting the canopy resistance to zero in the Penman-Monteith equation provides a good approximation of the evaporation rate from a completely wet canopy (Gash et al., 1980). This is likely a common condition in TMCFs. Also, our data does not allow to separate total incoming radiation into its direct and diffuse components. This implies that we are not considering the reach of diffuse radiation into the underlying canopy, which could enhance evaporation from the lower strata. However, there are two important considerations regarding evaporation during fog effects. First, in relative terms diffuse radiation becomes dominant over the direct radiation, but in absolute terms, total incoming radiation is reduced. Second, fog conditions imply water-saturated air that reflects in a very low VPD, and thus, evaporation is suppressed again limiting the impacts on ET. In addition, both the widely-used Penman-Monteith model and the canopy rainfall interception model assume a single-layered canopy. Thus, the impact of diffuse radiation can only be evaluated with a vertically distributed canopy model. However collecting the information required to constrain such a model was beyond the scope and possibilities of the current study. The required expected net solar radiation at the study area was estimated from extra-terrestrial solar radiation derived from solar geometry (Donatelli et al., 2006) and the clear sky transmissivity was estimated through the Thornton and Running (1999) model. In addition, we estimated the PE quantiles and the mean seasonal differences from each AWS elevation.

2.2.3. Fog

Next to the rainfall gauges we set up a cylindrical Juvik type fog collector (Juvik and Nullet, 1995) with a diameter of 21 cm and height of 60 cm with a circular greenhouse UV resistant plastic of 141 cm diameter on top to avoid rainfall inputs but without avoiding wind driven drizzle (horizontal precipitation). Each fog collector had a funnel-hose-rubber lid connection to a Decagon ECRN-100 rainfall gauge. Data from each gauge were recorded at 10 min intervals on a Decagon EM50 data logger. All were positioned with the top at 2 m from the ground and were located on the side of the rainfall gauges avoiding up- and downwind positions in relation to the rainfall gauges. Data from fog collectors have to be interpreted with caution due to repeated failures in the connection system and occasional failures of the

rain gauges. Furthermore, since fog gauge performance depends on wind speed (Frumau et al., 2011; Villegas et al., 2008) and given the fact that the high elevation wind speed was less than half of the wind speed of the low elevation site (due to differences in upwind land cover, forest vs grassland; Ramírez et al., 2017a), we expect our measurements to underestimate the actual amount of water intercepted from fog. Therefore, our fog gauging system did not allow us to specifically quantify water inputs by fog. However, we aggregated our data to hourly intervals to discriminate between hours with and without fog (following Tanaka et al., 2011). We then used the hours with fog to establish the relation between fog occurrence and PE.

2.2.4. Through-fall data

We recorded TF data for OGFs using six stainless steel 'V' shaped troughs of 30 cm wide and 400 cm length. These troughs were set up in two groups of three troughs each. Within each group the troughs were placed at a minimum distance of 5 m from each other. For SECFs and EARFs we built 'U' shape troughs using half 10.4 cm diameter PVC pipes of 200 cm length. Three 'U' shape troughs were used for SECFs and two 'U' shape troughs for EARFs. Each trough was connected to a 6506H UNIDATA 50 ml tipping bucket. Data were recorded on Starlogger 6004D UNIDATA every ten minutes. To prevent clogging from leafs and other canopy debris we covered the troughs with a 3 cm eye plastic mesh. We did not quantify the splash effect of the mesh. However, the inclination of the troughs and the plastic material promoted the dripping of water into the trough. Troughs were cleaned every 15 days. Missing data due to system failures were excluded from the analyses. The percentage of missing data for OGFs was 9% (wet season = 11%, dry season = 7%), 8% (wet season = 10%, dry season = 4%) for SECFs, and 0.6% (wet season = 0.8%, dry season = 0) for EARFs. To include the forest cover heterogeneity we moved the troughs to different sites. Minimum time per site was one month and maximum time per site was 3 months. The shifting of the troughs was carried in one day for the setups in OGFs and another day for the setups in SECFs and EARFs. Maximum time between shifting OGFs' setups was one week before or after shifting SECFs' and EARFs' setups. TF data were always collected inside the studied forests and not close to any forest border nor on ridges (distance > 200 m). In the OGFs we sampled 60 different sites (70.9 m^2 of effective area), in SECFs we sampled 24 sites (4.8 m^2 of effective area) and in EARFs, we sampled 16 sites (3.3 m^2 of effective area). Every time the gauges were moved we estimated the troughs' inclination, as topography and rocky soils prevented from keeping these values constant, and performed the corresponding corrections to estimate the effective horizontal sampling area. Mean water depth to produce a tip for 'V' shaped troughs was 0.073 ± 0.001 mm and for 'U' shaped troughs was 0.422 ± 0.014 mm. The implications of these differences will be considered in the comparison of the inferred fog's effects for the high elevation OGF and low elevation SECF and EARF. We also kept the sites' disturbance to a minimum and checked the calibration of the tipping buckets. TF/P ratios were estimated by averaging TF data at each 10 min time step from all TF gauges in the same forest cover and excluding data when the gauges were failing. We then added all the averaged TF values and all the P values and estimated the TF_{total}/P_{total} per forest cover. We also estimated the median and corresponding error bounds from the TF/P ratios for each of the sampled sites to assess the variability as a function of forest cover and seasonality. The dry season corresponded to the months of December, January, February and March, whilst the wet season covered the remaining months, following the rainfall patterns described in the Study area Section (2.1). Error bounds give roughly a 95% confidence interval for the difference between two medians (McGill et al., 1978).

2.2.5. Canopy characteristics

We measured the Leaf Area Index (LAI) to evaluate differences between forest covers with a LAI-2000 Plant Canopy Analyzer (LI-COR) every 10 m along transects in each of the main forested covers (OGF = 186 data points, SECF = 182 data points, EARF = 117 data points). LAI was calculated by employing the LAI-2000 computing method programmed in the Li-COr's FV2000 software (http://envsupport.licor.com/docs/FV2000Manual.pdf). Along the same transects we also took hemispherical photographs to evaluate Vegetative Cover Fraction (VCF) differences between forest covers. These photographs were taken with a Sigma 8 mm f/3.5 EX DG circular fish-eye lens (180° field of view) mounted on a Canon EOS rebel Ti LSR camera. In addition, we measured VCF for each trough through hemispherical photographs taken from the troughs' centre point. The hemispherical photographs were processed with the CAN-EYE v6 3.13 software (Weiss and Baret, 2014). Photography processing included calibrating the camera-lens system according to the procedure described in the CAN-Eye software's manual, classifying the photograph pixels into canopy or open sky and establishing the proportion of canopy pixels. The classification threshold was established on a per photograph basis. Finally, we assumed no differences in leaf phenology throughout the study period, as we found no evidence of deciduous species in the study area. Any more subtle synchronization in leaf phenology of perennial species was not considered.

2.3. Rutter model parameterization and evaluation

The Rutter numerical rainfall interception model (Rm; Rutter et al., 1971, 1975) was originally developed to analyse rainfall interception on a Corsican pine forest but has been widely applied to various forest types worldwide (Muzylo et al., 2009). The Rm approach simplifies the canopy by representing it as a single or bulk canopy layer. This matches the extent to which the canopy water balance terms were measured. In this study we used Rm as a tool to integrate our data and to provide a better insight on the canopy interception process. More specifically, we used it to: a) identify periods during which the observed TF could not be attributed to rainfall; identified by a zero signal in the simulated TF, and b) to have an approximation of the effects of contrasting PE under varying fog conditions on actual evaporation and in the wet and dry canopy frequency. Furthermore, we excluded stemflow because previous studies have found stemflow to be generally low for TMCFs (1–2% of measured P; Bruijnzeel et al., 2011), likely due to the large storage capacity of epiphytes (Ah-Peng et al., 2017). The implications of this are further addressed in the discussion of our results.

In Rm, water input to the canopy is defined by the proportion of rainfall that is intercepted by the canopy (I in mm time $step^{-1}$). The proportion of rainfall that will pass through the canopy without being intercepted is defined by the open spaces of the canopy. A good approximation of open spaces in the canopy is 1-VCF (vegetative cover fraction) of the canopy (i.e. Gash et al., 1995). Consequently, the remaining rainfall proportion is assumed to be intercepted by the canopy. Water leaves the canopy by evaporation (E in mm per time step) and drainage (D in mm per time step; Table 1). In the original model version (Rutter et al., 1971) D is calculated from the amount of water stored in the canopy (C in mm), the drainage rate (D0 in mm per time step), the canopy water storage capacity (S in mm) and an empirical parameter (b; Table 1). A modification was later introduced in which D is set to 0 when $C < S$ to prevent drainage when C becomes 0 (Calder, 1977). We followed the suggestion by Rutter et al. (1971) to estimate C after drainage by integrating the drainage term and calculating the change in C due to drainage for each time step (Table 1). This model considers a linear relation between evaporation and the C/S ratio. When C is equal or larger than S, evaporation is equal to PE, but once C becomes less than S, PE is reduced as a function of the C/S ratio. However, conflicting evidence has emerged on this relationship (Klaassen, 2001). Schellekens et al. (1999), for example, found that both the Rutter and Gash models severely underestimated the observed interception loss, likely due to underestimating evaporation. Therefore, we modified the calculation of evaporation by applying a nonlinear relationship that results in an enhanced evaporation rate shortly after rainfall (Rm-E_{nl}; Table 1).

Table 1
Rutter model components and the evaporation modules. Rainfall (P; mm), Vegetative cover fraction (VCF), Intercepted rainfall (I; mm), Evaporation (E; mm), Potential Evaporation (PE; mm), Canopy stored water (C; mm), Canopy storage capacity (S; mm), Drainage (D; mm), Drainage rate when S = C (D0, mm time-step^{-1}), time-step (t; minutes), drainage parameter (b), through-fall (TF; mm).

	Rm
Intercepted rainfall	$I = P * VCF$
Linear Evaporation (E)	$E = PE * (C/S)$ when $C < S$ $E = PE$ when $C > S$
Modified non-linear evaporation (E_{nl})	$E_{nl} = PE* [2(C/S) - (C/S)^2]$ when $C < S$ $E_{nl} = PE$ when $C > S$
Drainage	$D = D0*e^{b(C-S)}$ when $C > S$ $D = 0$ when $C < S$
Integrated drainage over time steps. Water stored in the canopy after drainage for each time step	$C_{t1} = \ln(e_{t0}^{-bC} + tbD0*e^{-b*S})*-b^{-1}$
Change in the amount of water stored in the canopy	$dc/dt = I-E-D$
Through-fall	$TF = P*(1-VCF)+D$
S, D0 and b	Model parameters, identified by optimization of the NSE between observed and simulated TF, using the Levenberg-Marquardt optimization algorithm

From the required input variables to constrain the Rutter model, we measured P, TF and VCF, and estimated PE from the observed meteorological parameters. In addition, we estimated the three parameters (S, D0 and b) by optimizing the Nash-Sutcliffe Efficiency Index (NSE; Nash and Sutcliffe, 1970). The NSE is based on three components that represent the correlation between observed and simulated outcomes; the bias, and a measure of relative variability in the simulated and observed values (Gupta et al., 2009). The NSE can vary between minus infinity (extremely poor model performance) to plus 1 (model perfectly matches observations). Often, an NSE of > 0.6 is perceived as indicator for a behavioral model (e.g. Melsen et al., 2014; Pappenberger and Beven, 2004). In this study the NSE compares the observed and simulated TF at 10 min temporal resolution for observation periods without missing data. For the optimization of the NSE we used the Levenberg-Marquardt optimization algorithm (Levenberg, 1944; Marquardt, 1963; Table 1; Appendix A in Supplementary material) instead of the usually employed TF and P regression method (i.e. Jackson, 1975) because the regression method requires identifying a minimum rainfall intensity threshold to fill the canopy and a fairly arbitrary selection of a regression line on the upper bounds of the data dispersion. The optimization was performed for both Rutter model versions: Rm and Rm-E_{nl}. The error bounds for all comparisons between NSE and model parameters corresponded to the boxplot notches which give roughly a 95% confidence interval for the difference in two medians (McGill et al., 1978).

2.4. Impact of temporal resolution on fog water input estimate (RQ1)

TF data reported in the literature were collected at different temporal resolutions. This likely has a strong effect on the estimates of additional water inputs by fog. To evaluate this effect we first averaged the TF data per time-step among the troughs located in the same forest cover and then we aggregated the averaged 10 min data in hourly and daily time-steps for the shared time series between forest covers. The data time series were partitioned for each temporal resolution and forest cover between data when P > TF and data when TF > P (represented in the lower halves and upper halves, respectively, in the panels of Fig. 6; Appendix A). The difference between TF and P when TF > P was assumed to represent the additional water inputs by fog to the system (TF_{add}). Afterwards, we established the proportion of TF_{add} in relation to total measured P (P_{total}) for each temporal resolution. We also verified that the TF_{total}/P_{total} remained constant across the different temporal resolutions.

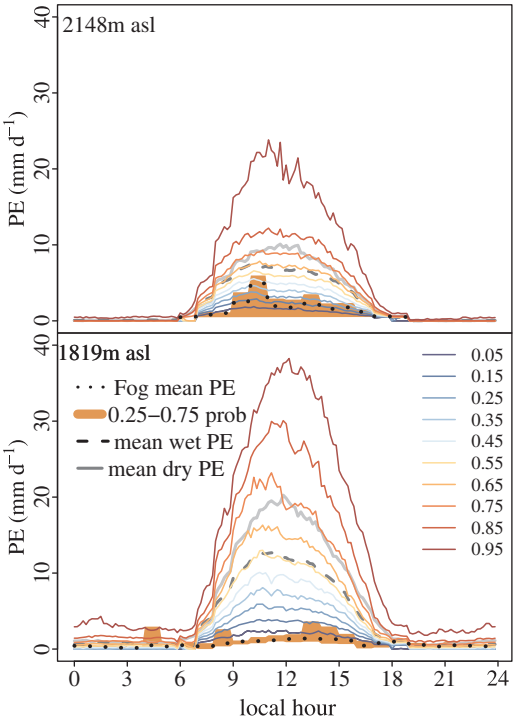

Fig. 3. Diurnal cycles of potential evaporation at two elevations. Top panel: potential evaporation at 2148 m asl, Bottom panel: potential evaporation at 1819 m asl. Potential Evaporation (PE) quantiles (mm d^{-1}) are estimated by the Penman-Monteith model. We also plotted the mean wet and dry season PE and the 0.25 and 0.75 PE quantiles during observed fog events.

2.5. Canopy water balance partitioning under different fog conditions (RQ2)

Evaporation depends on the amount of canopy water available to fulfil PE water demands and thus, it will also determine the dry and wet (dry/wet) canopy frequency. However, measuring evaporation and dry/wet canopy frequencies directly was not feasible due to the remote and steep character of the site, and budget limitations. Alternatively, Rutter model simulations can be used to estimate dry/wet canopy frequencies and also to assess the potential effect of higher (clear skies) and lower (overcast skies) solar radiation levels on the canopy water balance of each forest cover. Our approach therefore consisted of a sensitivity analysis performed by forcing the 0.5, 0.25, 0.55, 0.75 and 0.95 quantiles from the estimated PE time series (Section 2.2.2; Fig. 3) for the two studied elevations simulated with Rm-Enl for each site using the optimized parameters. We compared the simulated E/TF ratios and the dry/wet canopy frequency (dry when C = 0; wet when C > 0) within and between the forest covers (Appendix A). We also estimated the PE/TF ratio from our observed TF and estimated PE to use it as a reference value.

2.6. Fog water inputs from fog-only events (RQ3)

Fog events occurring without rainfall are not always detected by the fog gauges given their dependence on fog water content and wind speed (Villegas et al., 2008). Observed TF when there is no rainfall could represent the water inputs by fog events, but these TF observations could also be caused by canopy storage drip. Therefore, simulated TF can allow us to discriminate between fog drip events and canopy drainage after rainfall. For all sites we extracted the recorded fog drip

when the simulated TF was equal to zero to estimate the input of fog water and proportion of days with fog at the three forest covers. Given that TF gauges presented failures on different moments we excluded missing data from the daily mean estimates per forest cover. To estimate this mean monthly water inputs by fog we multiplied daily mean values of fog water input by the number of days per month, assuming that fog inputs during the days with observations were representative for the entire month (Appendix A).

2.7. Fog effects on through-fall during rainfall events (RQ4)

The co-occurrence of fog and rainfall is common in the Orinoco TMCFs (Ramírez et al., 2017a). This limits quantifying the fog effect on canopy interception. Usually, this effect is only quantified when TF exceeds P. However, this would neglect the effect of fog in reducing evaporation. This can lead to a persistently wet canopy (see Section 2.5) and those specific events where fog, despite contributing to fill the canopy water storage, does not necessarily cause TF to exceed P. This, either because the canopy storage is not completely full and/or because evaporation is also withdrawing water from the canopy. To detect the fog's influence during rainfall events we selected rainfall events that were preceded by three dry hours and that lasted for at least forty minutes. Then we evaluated the TF/P ratio at the first four ten-minute time steps of rainfall (40 min; t_0: from 0 to 10 min; t_1: from 10 to 20 min; t_2: from 20 to 30 min; t_3: from 30 to 40 min) between the wettest/foggiest months and the driest months for each of the forest covers, identified from Section 2.6 (Appendix A in Supplementary material). We excluded intermediate months from the analysis. We chose to evaluate the first 40 min of rainfall because the mean rainfall event duration in the area is slightly over 30 min. We also summarize in a table the rainfall intensity and PET during and previous to the evaluated rainfall events (Table 5). In Appendix B in Supplementary material we show the plot and the corresponding summary table of the same analysis but for rainfall events preceded by a six hour period without rainfall.

3. Results

3.1. Hydro-meteorology

3.1.1. Rainfall

Mean daily rainfall recorded at the high elevation (RS_{2148} = 13.9 ± 19.0 mm day^{-1}) was higher than the mean daily rainfall recorded at the lower elevation (RS_{1819} = 12.0 ± 18.9 mm day^{-1}) agreeing with the previously reported positive correlation along elevation (Ramírez et al., 2017a). During the wet season RS_{1819} recorded a lower mean daily rainfall (17.6 ± 21.8 mm day^{-1}) and slightly longer dry spells (< 0.2 mm h^{-1}; 7.6 ± 9.8 h) compared to RS_{2148} (18.3 ± 20.6 mm day^{-1} and 6.7 ± 6.8 h). These differences became larger during the dry season (RS_{1819}: 3.2 ± 7.3 mm day^{-1} and 22.8 ± 46.9 h; RS_{2148}: 4.8 ± 11.0 mm day^{-1} and 13.2 ± 12.0 h). This suggests that less severe dry season conditions occur at the higher elevation.

3.1.2. Meteorological data and PE estimates

The meteorological data from the two weather stations (AWS_{1819} and AWS_{2148}) indicate cooler and wetter conditions that lead to a lower estimated PE in the higher elevations compared to the lower elevations (Table 2).

Analysis of the seasonal mean differences showed that even though PE was higher in the dry season than in the wet season at both elevations, PE_{2148} showed less pronounced seasonal differences in comparison to PE_{1819} (Fig. 3). Fig. 3, also shows that the PE_{1819} quantiles were more evenly distributed compared to the PE_{2148} quantiles, where the occurrence of clear sky days were rare.

Table 2
Mean daily values (± sd) of meteorological data at the two Automated Weather Stations (AWSelevation in m asl) and PE estimates (mm y^{-1}) obtained by the Penman-Monteith model.

	AWS_{1819}	AWS_{2148}
Short-wave incoming solar radiation (W m^{-2})	134.1 ± 64.6	104.9 ± 48.6
Measured/expected clear-sky solar radiation	0.41	0.32
Relative humidity (%)	92.3 ± 4.6%	96.3 ± 3.9
Air temperature (°C)	16.6 ± 0.9	14.7 ± 0.8
Barometric pressure (kPa)	82.8 ± 0.3	79.9 ± 0.2
Wind speed (m s^{-1})	1.4 ± 0.4	0.6 ± 0.2

3.1.3. Fog

Fog occurrence measured by the fog gauge at the lower elevation showed that 75% of the daytime fog events were associated with inferred PE_{1819} values < 3.6 mm day^{-1} whereas night-time fog events mainly occurred at PE_{1819} values < 2.95 mm day^{-1} (Fig. 3). At the higher elevation the inferred PE_{2148} values during daytime fog events were higher (< 6 mm day^{-1}) compared to the lower elevation events, whilst we did not record any nocturnal fog event (Fig. 3), potentially due to low mean night-time wind speed (< 0.5 m s^{-1}; Ramírez et al., 2017a).

3.1.4. Mean observed through-fall to precipitation ratios

TF_{total}/P_{total} data revealed small differences between the forest covers. OGFs had the highest TF_{total}/P_{total} ratio (77%), followed by SECFs (74%) and EARFs (73%; Table 3) but median TF_{total}/P_{total} differences between forest covers indicate that these are not significant (OGFs = 77 ± 3%; SECFs = 68 ± 6%; EARFs = 69 ± 10%). Regarding seasonality, OGFs had the largest seasonal median differences (wet = 78 ± 5%; dry = 63 ± 8%) compared to SECFs (wet = 69 ± 4%; dry = 68 ± 4%) and EARFs (wet = 70 ± 10%; dry = 64 ± 34%). EARF's large error reflects the large variability in monthly TF_{total}/P_{total} during the dry season.

3.1.5. Canopy characteristics

Mean LAI was similar for OGFs and SECFs (4.8 ± 1.0 cm^2 cm^{-2} and 4.9 ± 0.8 cm^2 cm^{-2}, respectively). Mean measured EARFs' LAI was 4.0 ± 0.8 cm^2 cm^{-2}, slightly lower than OGFs' and SECFs' LAI. The measured distribution of VCF did not agree well with the measured LAI. In contrast to the LAI values for the three land covers, EARFs mean VCF (0.93 ± 0.05) was higher than OGFs (0.83 ± 0.10) and SECFs (0.87 ± 0.06). However, the standard deviation in the measured VCF from OGFs suggests that differences were not significant.

3.2. Rutter model evaluation

Despite the differences in the evaporation calculations between the two employed Rutter models (Table 1), both models performed equally well in terms of the NSE (Rm = 0.627 ± 0.053; Rm-E_{nl} = 0.628 ± 0.053). Therefore, model performance was not significantly improved by introducing the non-linear evaporation term introduced in Rm-E_{nl}. This is further illustrated in Fig. 4 which shows a comparison of the simulated and observed TF for three specific events for each forest cover type. In fact, simulation differences were almost imperceptible and there were no significant differences in the optimized median parameter values between models (Rm: S = 2.2 ± 1.2 mm; D0 = 0.39 ± 0.11 mm h^{-1}; b = 0.74 ± 0.14; Rm-E_{nl}: S = 1.5 ± 0.9 mm; D0 = 0.38 ± 0.19 mm h^{-1}; b = 0.72 ± 0.14).This result suggests that the model parameters can compensate each other and thus cannot easily be interpreted as physical properties. Furthermore, the selected specific events for each forest cover (7 h in total) shown in Fig. 4 also support a fairly good model performance based on a comparison with the observed TF. Given these results on model performance we selected the Rm-E_{nl} model for further analyses on the canopy water balance also because it considers the detected underestimated

Table 3
Temporal resolution effect on estimating additional water inputs for each forest cover. We partitioned P and TF time series per forest cover in different temporal resolutions (10 min, hourly and daily) in two groups: when P > TF (loss) and when TF > P (add). We show total P and TF amounts and their absolute difference for each group and the additional TF ratio (TF_{add}) to total measured rainfall (Pt). In the last column we present the TF_{total}/P_{total} ratio.

		10 minutes				hourly				daily				TF_{total}/P_{total}
		P (mm)	TF (mm)	abs diff	TF_{add}/P_t	P (mm)	TF (mm)	abs diff	TF_{add}/P_t	P (mm)	TF (mm)	abs diff	TF_{add}/P_l	
OGF	add	1244	2689	**1445**	**0.23**	1397	2202	**805**	**0.13**	821	998	**177**	**0.03**	**0.77**
	loss	5040	2131	**2909**		4892	2618	**2274**		5468	3821	**1647**		
SECF	add	1049	1926	**877**	**0.16**	827	1140	**313**	**0.06**	427	487	**60**	**0.01**	**0.74**
	loss	4314	2031	**2283**		4536	2817	**1719**		4936	3471	**1465**		
EARF	add	1185	2299	**1114**	**0.20**	1047	1503	**456**	**0.08**	714	815	**101**	**0.02**	**0.73**
	loss	4369	1734	**2635**		4507	2530	**1977**		4841	3218	**1623**		

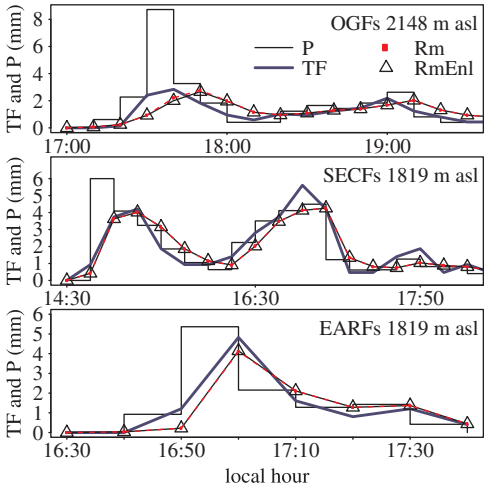

Fig. 4. Simulated and observed through-fall (TF) for three selected cases. Top panel: rainfall (P) recorded in old-growth forests (OGFs) in May 5, 2015. Middle panel: rainfall event recorded in secondary TMCFs (SECFs) in June 25, 2015; Bottom panel: rainfall event recorded in early succession TMCFs (EARFs) in May 5, 2015.Simulations are done using the standard Rutter model (Rm) and the Rutter model with non-linear evaporation ($Rm\text{-}E_{nl}$).

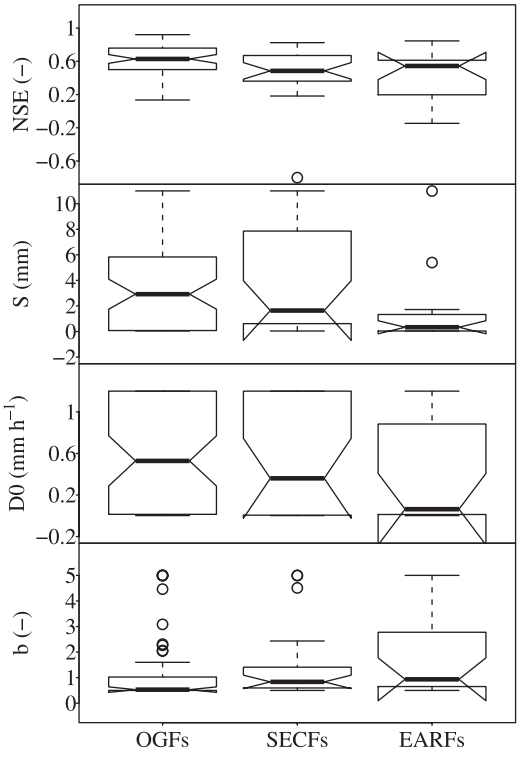

Fig. 5. Performance of the Rutter model and distribution of the optimized parameters. Model results are for the Rm model with non-linear evaporation for each land cover: OGF, SECF and EARF. From top panel to bottom panel: 1) Nash-Sutcliffe Efficiency Index-NSE; 2) canopy storage-S; 3) drainage at saturation-D0; and 4) drainage parameter-b.

evaporation by the Rutter model (Schellekens et al., 1999).

The median NSE obtained for the $Rm\text{-}E_{nl}$ simulations in OGFs was higher (0.628 ± 0.053) than for the simulations in SECFs (0.485 ± 0.010) and in EARFs (0.544 ± 0.164; Fig. 5). The inferred parameter values for OGFs (S = 2.92 ± 1.17 mm; D0 = 0.53 ± 0.24 mm h^{-1}; b = 0.53 ± 0.11) and SECFs (S = 1.64 ± 2.33 mm; D0 = 0.36 ± 0.39 mm h^{-1}; b = 0.83 ± 0.26) suggest that the dynamics in canopy rainfall interception for these two forest covers is very similar with larger storage and drainage rates compared to EARFs low S and D0 estimates (S = 0.33 ± 0.51 mm; D0 = 0.06 ± 0.34 mm h^{-1}; b = 0.93 ± 0.83; Fig. 5).

3.3. Impact of temporal resolution on fog water input estimates (RQ1)

Analysis of data aggregation to coarser temporal resolutions shows that there is generally a decrease in the monthly and total TF_{add}/P_{total} ratio and an increase in the intercepted rainfall in all forest covers (Fig. 6 and Table 3). The differences in estimated TF_{add}/P_{total} comparing the 10 min and the daily temporal resolution data for the different forest covers were 0.2 in OGFs (10 min TF_{add}/P_{total} = 0.23), 0.15 in SECFs (10 min TF_{add}/P_{total} = 0.16) and 0.18 in EARFs (10 min TF_{add}/P_{total} = 0.20). Expressed in absolute rainfall amounts these values translate into considerable TF_{add} differences of 1268 mm in OGFs, 817 mm in SECFs and 1013 mm in EARFs (Table 3). Therefore, when using longer temporal resolutions most additional water inputs become unnoticeable (< 0.03). Monthly total additional water inputs by fog using the hourly temporal resolution ranged between 5% and 25% of total monthly rainfall in OGFs, between 2% and 12% in SECFs and between 2% and 19% in EARFS.

3.4. Canopy water partitioning under contrasting PE conditions (RQ2)

The observed TF values were typically lower than the simulated TF (Fig. 7). This can be caused by multiple reasons: an underestimation of evaporation by the model and not accounting for the effect of diffuse radiation under foggy conditions, ignoring the role of stemflow or missing sources of water, caused by an overflow of the tipping bucket before or during tipping, especially under high-intensity rainfall. However, fog's relative influence in the canopy water balance was determined by forcing the inferred quantile range of PE for each elevation (from clear skies conditions to foggy days) in the $Rm\text{-}E_{nl}$ model and partitioning rainfall inputs into TF and E and determining the dry/wet canopy frequency for each forest cover (Fig. 7). The increase in the simulated E/TF median from the 0.05 PE quantile (PE under foggy conditions) to the 0.95 PE quantile (clear skies) was 0.21 for OGFs, 0.25

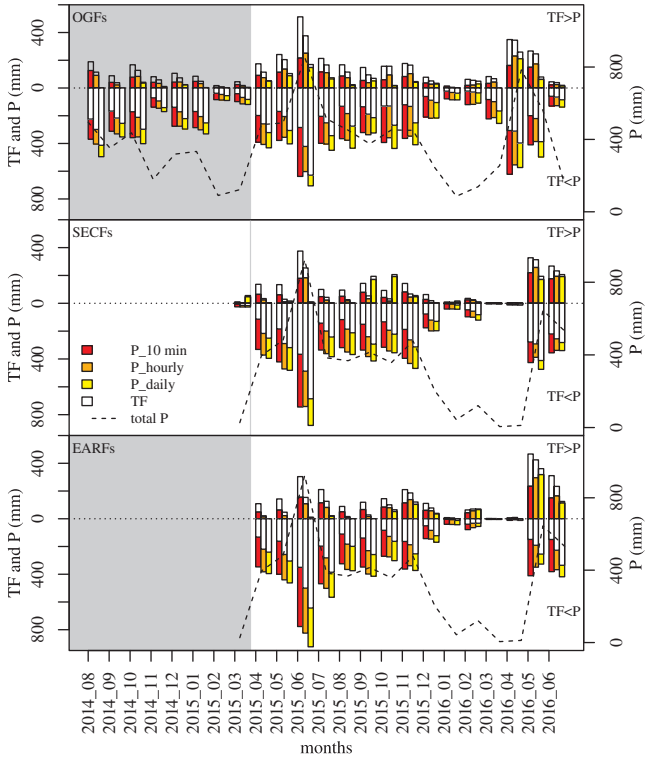

Fig. 6. Separation of rainfall events into those with lower through-fall (TF) than rainfall (P) and those with higher TF than P at different temporal resolutions. Data is shown in monthly totals. The evaluated temporal resolutions were: 10 min, hourly and daily. Data plotted in the bottom half of each panel is when P exceeded TF and data plotted in the upper half of each panel is when TF exceeded P. Top panel: Old-growth TMCF (OGF), middle panel: Secondary TMCF (SECF), and bottom panel: Early succession TMCF (EARF). Total monthly P is on the right side axis. The grey area represents the OGF's and SECF's data excluded from the analysis in Table 3.

for SECFs and 0.17 for EARFs. The similar increase in E/TF for OGFs and SECFs did not reflect the strong PE differences with elevation (c.f. Fig. 3). The inferred larger difference in E/TF between SECFs and EARFs, both exposed to similar meteorological conditions, was more related to differences in the canopy storage (Fig. 7). This was further supported by the dry/wet canopy analysis in which EARFs had a longer dry canopy frequency than SECFs for all analyzed PE quantiles. Therefore, EARF's drier canopy implies that E was reduced because it did not have available water to fulfil the PE demands.

3.5. Fog water inputs by fog-only events (RQ3)

The model simulations were used to separate drainage after rainfall from fog drip caused by interception. This allows to quantify the fog water inputs by fog-only events and address our third research question. Results indicated differences in fog water inputs by fog-only events between forest covers (Fig. 8). These differences have an associated uncertainty due to differences in the minimum tipping water depth of the TF gauges in OGF (0.07 mm tip^{-1}) and SECF/EARF (0.4 mm tip^{-1}). TF gauges in OGF are more sensitive to fog inputs and have a lower influence of residual water stored in the tipping bucket from previous rainfall, whereas TF gauges in SECF and EARF are less sensitive to fog inputs and have a larger influence of residual water (from 0.00 to 0.39 mm) stored in the tipping bucket from previous rainfall. However, a random distribution of residual water in the TF gauges can be safely assumed throughout the study period and between gauges. Days with fog-only events were on average more frequent at OGFs than at SECFs and EARFs, except during the dry season. However, the measurement records for SECFs and EARFs were shorter than for OGFs preventing us from comparing the fog inputs on the 2014–2015 dry season. According to both rainfall and PE data the 2015–2016 measured dry season was evidently more severe than the 2014–2015 dry season. This is likely due to the influence of the strong 2015–2016 El Niño event (Jiménez-Muñoz et al., 2016; Fig. 8). Nevertheless, at least for the strong dry season, fog-only water measurements suggested a lowering in the condensation level increasing the inputs of fog water at the lower elevation forest sites. In relation to water inputs by fog from fog-only events, OGFs showed a range between 0.2 mm month^{-1} in the driest months to more than 20 mm month^{-1} during the wettest month. Throughout the study period from August 2014 to May 2016 (22 months) OGFs had 147.3 mm of water inputs by fog drip (equal to 80 mm y^{-1}), representing 1.6% of the total water inputs (9313 mm). Monthly water inputs in OGFs by fog-only events ranged between 0.02% and 7% of monthly rainfall. SECFs tended to have slightly higher fog inputs than EARFs, but even in the months with higher fog inputs, this never exceeded 10 mm month^{-1}. Throughout the study period total fog inputs from fog-only events for SECFs and EARFs (April 2015 to May 2016, excluding April 2016) were 79.5 mm and 45.4 mm. This represents 1.5% and 0.8% of the total water inputs (5363 mm and 5554 mm), respectively. Monthly water inputs by fog-only events ranged between 0.6% and 11% of total monthly rainfall in SECFs and between 0 and 5% in EARFs. However, there is no coincidence between OGF and SECF or EARF in the months with the highest fog water inputs. In terms of seasonality, OGFs fog inputs were related to monthly rainfall, but the months with highest rainfall were not necessarily the months with higher fog frequency or inputs (Fig. 8). Overall, our estimates on fog water inputs by fog interception are conservative given that we are only considering water inputs from fog-only events and exclude fog water inputs during rainfall events.

3.6. Fog effects on through-fall during rainfall events (RQ4)

In the previous section we only quantified the fog that dripped from the canopy after filling the canopy storage. In this section, we approach our fourth research question by quantifying the effect of fog on TF caused by fog's effect on sustaining wet canopies through a reduced evaporation and by partially filling the storage during the first forty minutes of rainfall. For this approach we chose the foggiest and least foggy months according to the analysis of the data from the previous section (Table 4).

As rainfall progressed there was a gradual increase in the TF/P proportion for all forest covers as expected by the gradual saturation of the canopy water storage, including tree trunks and leaves, and epiphytes (Fig. 9). In OGFs the contrasts in the median TF/P between rainfall events during the least foggy months ($t_2 = 0.23 \pm 0.05$; $t_3 = 0.36 \pm 0.07$) and the foggiest months ($t_2 = 0.37 \pm 0.06$; $t_3 = 0.64 \pm 0.08$) were strongly significant (*sensu* Chambers et al., 1983). Even though there were rainfall events in both the foggiest and less foggy months when TF largely exceeded P, these were most common during t_3 in the foggiest months (Fig. 9). In the case of SECFs, median differences in TF/P between the foggiest months and the least foggy months became significant only after 30 min (t_3) of rainfall (foggiest months = 0.70 ± 0.12; least foggy months = 0.19 ± 0.20). In the case of EARFs, no significant evidence of fog influence was observed in the TF/P ratio when comparing foggiest with least foggy months. The results for the analysis of rainfall events with a previous dry period of six hours are shown in Appendix B as Supplementary material because they were very similar to those of the rainfall events with a previous dry period of three hours.

Table 5 lists the means and standard errors of P intensities and PE values of both the foggiest (wet) and least foggy months (dry) to evaluate if they can influence the TF/P differences described previously. In OGFs, differences in P intensities were smaller than the error bounds, except in the first 10 min when P was highest in the least foggy month compared to the foggiest month. Differences in PE during

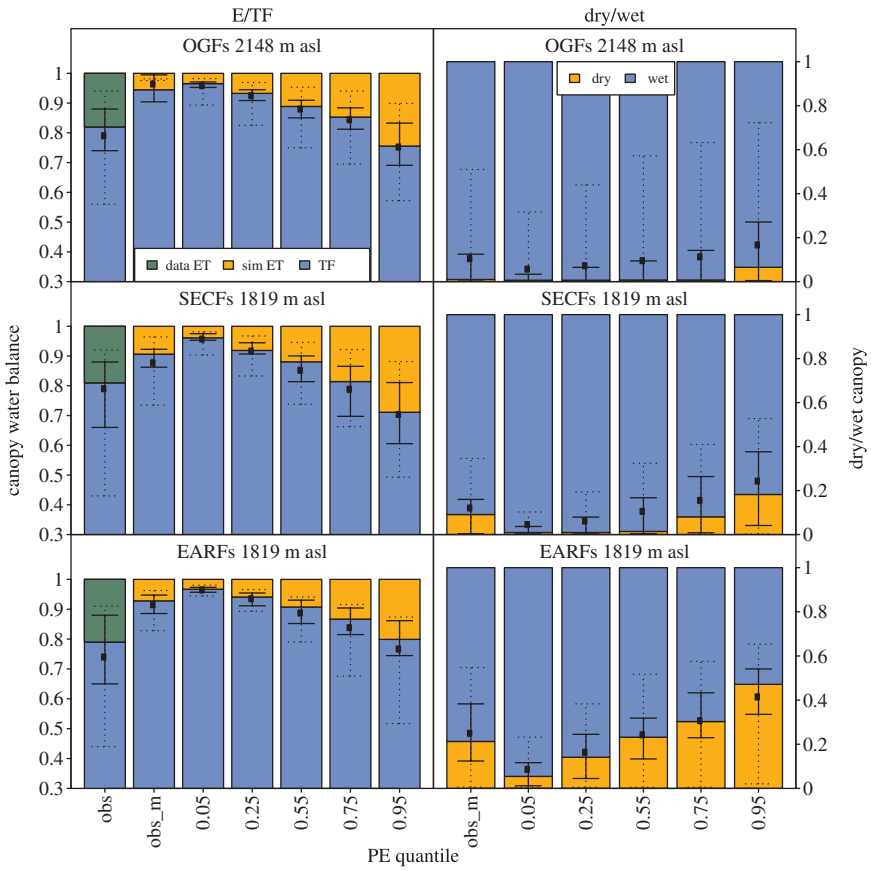

Fig. 7. Influence of fog on the water balance partitioning into median through-fall and evaporation and dry/wet canopy frequency. Results originate from simulations employing estimated potential evaporation (PE) for the observed meteorological time series (obs_m), and simulations forced with the PE quantiles from higher to lower fog influence (0.05, 0.25, 0.55, 0.75,0.95; x-axes). Plots on the left show the simulated evaporation/through-fall ratio (E/TF; orange/blue) and plots on the right show the simulated canopy dry/wet frequency (orange/blue). The measured water balance in terms of PE (in green) and TF (blue) is also shown. Solid error bars are the 0.25 and 0.75 of the distribution and dotted error bars are the 0.05 and 0.95 of the distribution. The dots represent the mean values. Top panels: High elevation old-growth forest (OGF 2148 m asl); middle panels: Low elevation secondary TMCF (SECF 1819 m asl); and bottom panels: Low elevation early succession TMCF (EARF 1819 m asl) (For interpretation of the references to colour in this figure legend, the reader is referred to the web version of this article).

rainfall were not significantly different whereas antecedent PE_{1h} and PE_{dry} were higher in the least foggy months. Higher antecedent PE leads to drier canopies, thus influencing the TF/P values. In SECFs, P_{t0} differences between the foggiest and least foggy months were smaller than the error bounds. Afterwards, P_{t1} and P_{t2} had higher values in the foggiest months, and P_{t3} was larger in the least foggy months. These P variations are not reflected in the TF/P patterns depicted in Fig. 9. Differences in PE during the preceding dry period between the foggiest months and the least foggy months varied. Whilst PE_{1h} was higher in the foggiest months, PE_{dry} was higher in the least foggy months. In this case, PE_{dry} can be more relevant for reducing the water stored in the canopy and thus influencing observed TF/P differences. Potentially wetter canopies can lead to the observed tendency of higher TF/P in the foggiest months. In EARFs, P_{t0} were higher in the least foggy months compared to the foggiest months, whereas differences in Pt_2 were larger in the least foggy months. These variations were not reflected in the observed TF/P patterns. In addition, PE differences were smaller than the error bounds, suggesting that PE was not relevant to explain the observed TF/P ratios.

4. Discussion

The overall evaluation of the canopy characteristcs and the TF_{total}/P_{total} values for the studied forest covers were comparable to those reported in other studies in TMCFs. Regarding the canopy, the LAI values for both SECFs' and OGFs' canopies (4.8 ± 1.0 $cm^2\ cm^{-2}$ and 4.9 ± 0.8 $cm^2\ cm^{-2}$, respectively) resembled the lower montane cloud forest mean values (4.7 ± 1.1 $cm^2\ cm^{-2}$; Bruijnzeel et al., 2011). This similarity in LAI estimates between OGFs and SECFs is a common observation in tropical forests (e.g. Brown and Lugo, 1990), including TMCFs, where LAI recovery can be relatively fast attaining 50% of the original forest LAI values after only three years (Lawton and Putz, 1988). This also explains the fairly high LAI value for EARFs (4.0 ± 0.8 $cm^2\ cm^{-2}$). The larger VCF values in EARF (0.93 ± 0.05) in comparison to the other two forest covers (OGFs = 0.83 ± 0.10; SECFs = 0.87 ± 0.06), albeit not being significant, corroborate that canopy gaps can increase with stand age (Brown and Lugo, 1990; Clark, 1996) and forests subjected to selective logging, such as the OGFs in the study area, are expected to have more canopy gaps (Clark, 1996).

In terms of the TF_{total}/P_{total} ratios, the values in OGF's (77%) were close to the mean TF of 81 ± 11% reported by Bruijnzeel et al. (2011) for lower montane cloud forests. SECFs' TF_{total}/P_{total} values (74%) agreed with the 75% reported by Hölscher et al. (2011) for mid successional TMCFs but were lower than the > 80% reported for the Mexican secondary TMCFs (Holwerda et al., 2010). In the case of EARFs the TF_{total}/P_{total} values were in between those reported in the literature. To our knowledge, only Hölscher et al. (2011) and Pryet et al. (2012) have reported TF/P observations for early successional/shrubby TMCFs. Their mean TF/P ratios for early successional TMCFs are very different: 115% in Pryet et al. (2012) and 69% in Hölscher et al. (2011). Despite agreeing with the values reported in other studies, these results do not provide information on the potential amounts of additional water inputs by fog. Furthermore, the fairly large variation in PE values that were related to fog occurrence in the study area (see Section 3.1.2) corroborate the elusiveness of the fog signal as a function of insolation and/or relative humidity (Brauman et al., 2010).

The interaction between the vegetation and the atmosphere in TMCFs is modulated by multiple processes that are highly sensitive to fog. Despite that the fog's influence on canopy interception is widely acknowledged, quantifying its effects has been generally approached following a 'black-box' or input/output approach that neglects these processes. Thus, we analyzed the fog's influence on each process separately, namely evaporation (RQ2), and fog interception during fog-only events (RQ3) and during foggy rainfall events (RQ4; Fig. 1). While our analysis is based on TF data, we employed the Rutter model to infer canopy water storage dynamics. The Rutter model generally performed

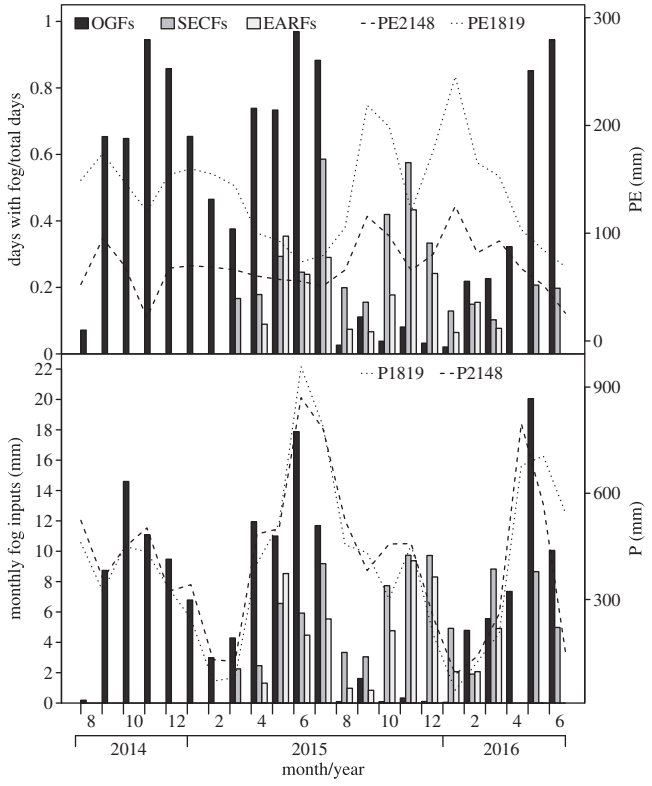

Fig. 8. Through-fall due to fog. The top panel shows the monthly proportion of days with fog occurrence at each main forest covers (OGF, SECF and EARF) and the monthly potential evaporation (PE) estimated at both elevations: 2148 m asl and 1819 m asl. The bottom panel shows monthly fog inputs and rainfall measured at 1819 m asl and 2148 m asl. Note that data for OGF was collected from August 2014, whilst data for SECF and EARF was collected from in April 2015, and had no data on April 2016. Data for all forest covers were collected until June 12, 2016.

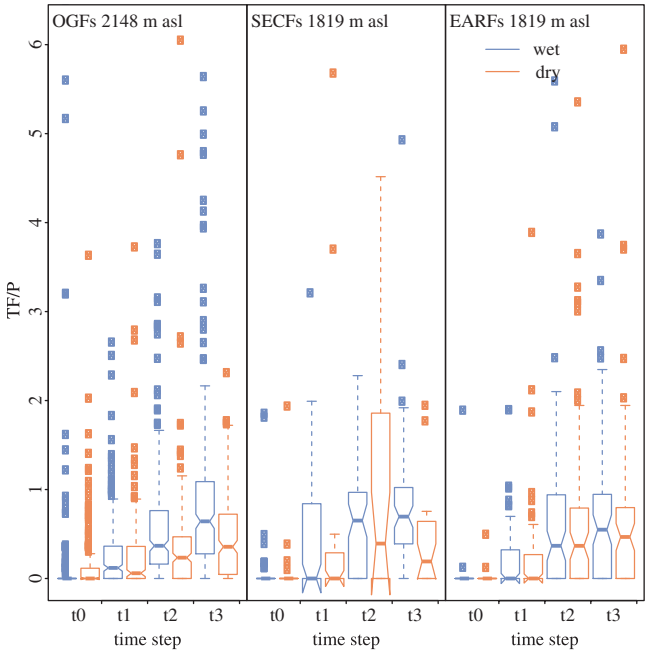

Fig. 9. Evolution of through-fall/rainfall ratios in the foggier and least foggy months during onset of rainfall. Left panel: old growth TMCF (OGF), middle panel: secondary TMCF (SECF) and right panel: early succession TMCF (EARF). Time steps indicate the first four 10 min time steps of each rainfall event.

Table 4
The foggiest and least foggy months (MFM and LFM) chosen per forest cover (Old-growth TMCF-OGF; Secondary TMCF-SECF; Early succession TMCF-EARF) for the analyses on the fog effects during rainfall.

	Selected Months
OGF - MFM	Oct-2014, Nov-2014, Apr-2015, May-2015, Jun-2015, Jul-2015, May-2016, Jun-2016
OGF - LFM	Aug-2014, Aug-2015, Sep-2015, Oct-2015, Nov-2015, Dec-2015, Jan-2016
SECF - MFM	Jul-2015, Oct-2015, Nov-2015
SECF - LFM	Sep-2015, Jan-2016, Feb-2016, Mar-2016
EARF - MFM	May-2015, Jul-2015, Nov-2015, Dec-2015
EARF - LFM	Aug-2015, Aug-2015, Jan-2016, Mar-2016, May-2016

well, but the estimates of the parameter values (S, D0 and b) constrained only by TF data do not necessarily represent the physical canopy characteristics they intend to due to their compensatory character (Vrugt et al., 2003). Also, fog presence is expected to influence the estimation of the canopy storage (S). Fog presence increases water interception by the leaves, so we are quantifying its output (in TF) but not its input, thus the Rutter model can assume either a lower storage capacity or a faster drainage rate. Therefore, using these inferred parameter values to define and compare canopy characteristics of different forests (or studies) can be misleading. However, the running water balance principle of the Rutter model suggest that the water storage and release from the canopy is properly represented, and thus, it can provide insights on the canopy water dynamics.

Another important factor when evaluating the canopy water balance of TMCFs from TF observations is their temporal resolution. Water inputs by fog interception, identified when TF > P can be overestimated using high temporal resolution (< 10 min) that separate the canopy wetting (TF < P) and post rainfall dripping (TF > P) phases during P events. In contrast, using lower temporal resolutions (> day) underestimate fog water inputs by mixing rainfall events with and without fog, and fog-only events which can all happen within a day. Therefore, an intermediate temporal resolution (hourly) achieves a better compromise in aggregating rainfall-canopy phases and accounting for daily meteorological variations. The estimates of water inputs by fog interception in the hourly resolution (TF_{add}/P_{total}) ranged from 0.08 to 0.13 (Table 3). These numbers reflect fog effects on the canopy water balance only when TF > P, however, other fog effects might pass unnoticed with this approach.

The effect of fog on reducing actual evaporation (E) was further investigated by forcing on TF simulations the different quantiles of estimated PE from meteorological data. Contrasts in E/TF between foggy and fogless conditions ranged from 0.17 to 0.25 (Fig. 7). The canopy of OGFs had the lowest dry canopy frequency, thus, it tended to have enough available water to fulfil a fog-reduced PE (Fig. 3). This inferred dry canopy frequency agreed well with the observations in other fog affected forests (i.e. Chu et al., 2014) and this shows that the canopy (including associated epiphytes) requires long dry-spells of up to eight days to dry (Tobón et al., 2010; Mulligan et al., 2011). The relative rareness of having dry canopy conditions in OGFs and SECFs also indicates that there is a limited applicability of interception models that assume a dry canopy between rainfall events to study canopy water balances in TMCFs (e.g. the Gash model). At the other end, the canopy of EARFs was subjected to a higher PE and it was more frequently dry with the lack of available water in the canopy limiting E. The dryness of EARFs' canopies can be even more dramatic given the likely overestimation of rainfall interception due the potentially larger water amounts of water diverted to stemflow (4.5%; González-Martínez et al., 2017) that we did not quantify. Higher PE values increase E (OGFs vs SECFs), but if the canopy dries, E is reduced (SECFs vs EARFs). The higher water availability in the canopy of SECFs compared to EARFs' is most likely related to a more complex canopy with a higher epiphyte

Table 5
Seasonal and elevation differences in mean rainfall and mean potential evaporation of through-fall during analysed rainfall events at the three dominant forested land covers. Rainfall at the four analysed 10 min time steps (Pt_0 to t_3 in mm) and potential evaporation during the rainfall event (PE_{RF} in mm), one hour before the rainfall event (PE_{1h}) and for the whole dry period before the rainfall event (PE_{dry}).

	OGF 2148 m asl		SECF 1819 m asl		EARF 1819 m asl	
	Wet (n = 294)	Dry (n = 237)	Wet (n = 87)	Dry (n = 33)	Wet (n = 80)	Dry (n = 68)
Pt_0	0.66 ± 0.04	0.88 ± 0.06	0.86 ± 0.14	0.79 ± 0.19	0.68 ± 0.08	0.96 ± 0.16
Pt_1	1.84 ± 0.13	1.74 ± 0.13	1.97 ± 0.26	1.02 ± 0.16	1.74 ± 0.22	1.77 ± 0.23
Pt_2	2.09 ± 0.15	2.02 ± 0.15	1.94 ± 0.24	1.17 ± 0.31	2.11 ± 0.22	1.53 ± 0.18
Pt_3	1.68 ± 0.13	1.61 ± 0.15	2.34 ± 0.30	4.07 ± 0.84	2.50 ± 0.34	2.18 ± 0.36
PE_{RF}	0.033 ± 0.005	0.032 ± 0.01	0.07 ± 0.01	0.04 ± 0.01	0.034 ± 0.004	0.040 ± 0.005
PE_{1h}	0.073 ± 0.002	0.083 ± 0.002	0.12 ± 0.01	0.06 ± 0.02	0.06 ± 0.01	0.07 ± 0.01
PE_{dry}	0.50 ± 0.03	1.06 ± 0.08	1.50 ± 0.15	2.64 ± 0.42	1.60 ± 0.30	1.4 ± 0.16

load in more developed secondary forests. Furthermore, in terms of the canopy energy budget, the transition from a wet to a dry canopy increases the sensible heat fluxes (e.g. Holwerda et al., 2016; Ray et al., 2006). This is particularly important in TMCFs when considering the downwind effects of these energy fluxes to favour fog conditions (Lawton et al., 2001).

The analyses to quantify fog inputs showed that fog drip during fog-only events do not represent a significant input to the catchments' water budgets (from 0.8 to 1.6% of measured P; Fig. 8 and Fig. 10). These values are similar to the 1.4% reported in the relatively less exposed Jamaican forests (Hafkenscheid, 2000), to the fog contribution of 0.8% in Peruvian TMCFs (Gómez-Peralta et al., 2008) and to the < 2% in Mexican TMCFs (Holwerda et al., 2010). However, fog's contribution to through-fall during rainfall events is likely more relevant. For example, in OGF, TF/P after 30 min of rainfall was 0.28 to 0.51 times higher in the foggiest months than in the least foggy months (Fig. 9). Furthermore, the median TF/P values for all forest covers in both the foggiest and least foggy months were below the 1:1 TF/P ratio. This implies that this fog effect would pass unnoticed with the usual TF/P per rainfall event approach that only considers a fog influence for those events where TF exceeds P. However, our approach does not allow to estimate total fog inputs during all rainfall events. Thus, the uncertainty around these estimates remains considerable. For example, if we assume that the minimum estimated fog inputs were those derived from fog-only events and the maximum fog inputs are likely those estimated when TF > P in the hourly time resolution (Table 3), the potential range in total water inputs by fog relative to total rainfall for each forest cover is: 1.7% to 12.8% in OGFs; 1.5% to 5.8% in SECFs, and 0.8% to 8.2% in EARFs (Fig. 10).

In the case of high elevation OGFs, where fog tended to follow the seasonal rainfall (Fig. 8), the potential underestimate of water inputs to these TMCFs is only relevant during the wet season. This contrasts to other TMCF under oceanic influence, where fog water inputs are highly relevant during the dry season (e.g. Goldsmith et al., 2013). A larger water contribution by fog in the low elevation SECFs and EARFs compared to the high elevation OGFs during the sampled dry season, suggests a seasonal downward shift of fog along the elevation gradient (Fig. 8). However, with only one year of data we cannot know if this is a typical dry season phenomena, especially considering that the dry season intensity is highly variable between years (Ramírez et al., 2017b). Nevertheless, fog inputs are likely too low to explain the reported missing water inputs in the dry season (Ramírez et al., 2017a).

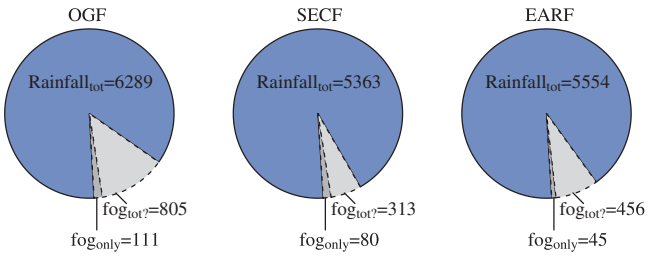

Fig. 10. Contribution of fog to total water input over the study period. Each pie-chart shows: estimated fog inputs during fog only events (fog_{only}; Section 3.5); maximum potential fog inputs estimated from the hourly time resolution when TF is larger than P ($fog_{tot?}$; Section 3.3), which include the fog_{only} inputs; and total measured rainfall ($Rainfall_{tot}$). Units are mm totals over the shared study period for all forest covers (April 1, 2015 to June 12, 2016).

From a catchment perspective, the fog effects we have described suggest that the higher elevations sustain overall wetter conditions in contrast to lower elevations subjected to a relatively smaller influence of fog. A higher moisture in the system can potentially translate into a larger contribution of water to streamflows. Even though additional fog water inputs represented a low proportion of total rainfall similar to other TMCFs (e.g. Holwerda et al., 2010; Hafkenscheid, 2000; Gómez-Peralta et al., 2008), fog plays a key role in enhancing TF during foggy rainfall events and in reducing PE, and thus E and transpiration. The reduction of evaporation leads to a frequently wet canopy, with important ecological implications given that TMCF plant species are highly vulnerable to dry atmospheric conditions (Oliveira et al., 2014).

The individual processes that have been evaluated in detail in this study have associated uncertainties that together explain the difficulty to close a water budget in TMCF catchments (e.g. Ramírez et al., 2017a; Clark et al., 2014; Muñoz-Villers et al., 2012). First, with only two measurement sites to provide the observations to infer PE along the elevation gradient we can only assume a linear dependence of PE along elevation. Second, we simplified forest covers in three major categories that are likely far from being homogeneous. A more detailed canopy characterization of the different forest covers, with the collection of micrometeorological data along the vertical gradient and stemflow data would allow to use more realistic, albeit complex, canopy interception and potential evaporation models suitable for multilayered canopies. However, this also requires more sophisticated experimental setups that are not easy to install and maintain in TMCFs which are often remote and inaccessible. Given the current concerns about climate and water availability changes in time, it is perhaps more pertinent to have simpler, more robust and affordable monitoring systems that can stay operational for longer time periods, such as meteorological ground stations and soil moisture sensors, rather than high-maintenance, high-cost equipment such as (micro)meteorological towers.

5. Conclusions

Quantifying the effects that fog has on the canopy water budget from through-fall (TF) data is highly challenging. However, depending on the temporal resolution of the observations, first order estimates are achievable. Our analysis showed that using 10 min resolution data instead of daily resolution data (RQ1) can increase by up to 20% the estimates of water inputs by fog. Data collected in daily or longer time periods average out fog effects by combining foggy and clear sky

conditions. This is an important consideration when comparing fog's influence across TMCFs that were studied based on datasets using different temporal resolutions.

We then evaluated fog's influence on each process separately, namely evaporation (RQ2) and fog interception during fog-only events (RQ3) and during foggy rainfall events (RQ4). Fog water inputs from fog only events represent a very low percentage of total rainfall (1.6% max). However, our results demonstrate that fog effects on the canopy water balance are in fact important to sustain the hydrology of TMCFs. For example, fog reduces the E/TF ratios by 25%. We also showed that TF is significantly enhanced during rainfall events co-occurring with fog, despite the fact that these events are not always associated with TF being higher than P. Therefore, studies that only account for the fog effects when TF exceeds P underestimate fog inputs. A reduction in fog persistence would not only have an impact on the amount of water reaching the ground but also on the canopy energy budget.

Extrapolating these evaluated effects of fog on the canopy water budget to the overall TMCF catchment water budget remains challenging due to associated uncertainties in the data collection system and analysis, and in the extrapolation of the point measurements to the catchment scale. Nevertheless, results show that higher elevations likely provide a larger contribution of water to streamflow due to stronger fog effects than the forests in the low elevations. In this way, our observations contribute to ongoing efforts to unravel and close the water balance of TMCF catchments.

Acknowledgements

This contribution is part of the first author's Doctoral thesis undertaken at Wageningen University, with a fellowship provided by Colciencias (Colombian Department for the Administration of Science, Technology and Innovation; Call 529-2011). This project was partially funded by Equion Energy Limited, Colombia (Solped: 14-01-2014-4000000215) and the Municipality of Chámeza, Colombia (Cooperation agreement 004-2014). We thank the two anonymous reviewers for their comments, which helped improve the manuscript, and appreciate Wilma Jans and Jan Elbers both from Alterra for their technical support and the Chamezan community for their constant interest and support during the field campaigns.

Appendix A. Supplementary data

Supplementary material related to this article can be found, in the online version, at doi:https://doi.org/10.1016/j.agrformet.2018.05.016.

References

Ah-Peng, C., Williamson-Cardoso, A., Flores, O., West, A., Wilding, N., Strasberg, D., Hedderson, T.A.J., 2017. The role of epiphytic bryophytes in interception, storage, and the regulated release of atmospheric moisture in a tropical montane cloud forest. J. Hydrol. 548, 665–673.
Balthazar, V., Vanacker, V., Molina, A., Lambin, E.F., 2015. Impacts of forest cover change on ecosystem services in high Andean mountains. Ecol. Indic. 48, 63–75.
Bonell, M., 2010. The impacts of global change in the humid tropics: selected rainfall-runoff issues linked with tropical forest-land management. Irrig. Drain. Syst. 24, 279–325.
Brauman, K.A., Freyberg, D.L., Daily, G.C., 2010. Forest structure influences on rainfall partitioning and cloud interception: a comparison of native forest sites in Kona, Hawai'i. Agr. For. Meteorol. 150 (2), 265–275.
Brown, S., Lugo, A.E., 1990. Tropical secondary forests. J. Trop. Ecol. 6 (01), 1–32.
Bruijnzeel, L.A., Eugster, W., Burkard, R., 2006. Fog as a hydrologic input. Encyclopedia of Hydrological Sciences.
Bruijnzeel, L.A., Mulligan, M., Scatena, F.N., 2011. Hydrometeorology of tropical montane cloud forests: emerging patterns. Hydrol. Process. 25 (3), 465–498.
Calder, I.R., 1977. A model of transpiration and interception loss from a spruce forest in Plynlimon, central Wales. J. Hydrol. 33 (3-4), 247–265.
Cantillo, E.E., Rangel, J.O., 2008. Aspectos de la estructura y del patrón de riqueza de la vegetación del transecto Sumapaz (Cordillera Oriental de Colombia). In: van der Hammen, T. (Ed.), La Cordillera Oriental Colombiana Transecto Sumapaz. Schweizerbart Science Publishers, Stuttgart, Germany, pp. 529–563.
Chambers, J.M., Cleveland, W.S., Kleiner, B., 1983. Graphical Methods for Data Analysis. Wadsworth International Group, Belmont.
Chu, H.S., Chang, S.C., Klemm, O., Lai, C.W., Lin, Y.Z., Wu, C.C., Lin, J.Y., Jiang, J.Y., Chen, J., Gottgens, J.F., Hsia, Y.J., 2014. Does canopy wetness matter? Evapotranspiration from a subtropical montane cloud forest in Taiwan. Hydrol. Process. 28 (3), 1190–1214.
Clark, D.B., 1996. Abolishing virginity. J. Trop. Ecol. 12 (05), 735–739.
Clark, K.E., Torres, M.A., West, A.J., Hilton, R.G., New, M., Horwath, A.B., Fisher, J.B., Rapp, J.M., Robles Caceres, A., Malhi, Y., 2014. The hydrological regime of a forested tropical Andean catchment. Hydrol. Earth Syst. Sci. 18, 5377–5397.
Crockford, R.H., Richardson, D.P., 2000. Partitioning of rainfall into through-fall, stemflow and interception: effect of forest type, ground cover and climate. Hydrol. Process. 14 (16–17), 2903–2920.
DeFries, R., Eshleman, K.N., 2004. Land-use change and hydrologic processes: a major focus for the future. Hydrol. Process. 18, 2183–2186.
Dietz, J., Leuschner, C., Hölscher, D., Kreilein, H., 2007. Vertical patterns and duration of surface wetness in an old-growth tropical montane forest. Indonesia. Flora 202 (2), 111–117.
Donatelli, M., Carlini, L., Bellocchi, G., 2006. A software component for estimating solar radiation. Environ. Model. Softw. 21, 411–416.
Eller, C.B., Burgess, S.S.O., Oliveira, R.S., 2015. Environmental controls in the water use patterns of a tropical cloud forest tree species, Drimys brasiliensis (Winteraceae). Tree Physiol. 35, 387–399.
Ellison, D., Futter, M.N., Bishop, K., 2012. On the forest cover-water yield debate: from demand- to supply-side thinking. Glob. Chang. Biol. 18, 806–820.
Ellison, D., Morris, C.E., Locatelli, B., Sheil, D., Cohen, J., Murdiyarso, D., Gutierrez, V., Van Noordwijk, M., Creed, I.F., Pokorny, J., Gaveau, D., 2017. Trees, forests and water: cool insights for a hot world. Global Environ. Chang. 43, 51–61.
Fleischbein, K., Wilcke, W., Goller, R., Boy, J., Valarezo, C., Zech, W., Knoblich, K., 2005. Rainfall interception in a lower montane forest in Ecuador: effects of canopy properties. Hydrol. Process. 19 (7), 1355–1371.
Førland, E., Hanssen-Bauer, I., 1996. Manual for Operational Correction of Nordic Precipitation Data. DNMI Report.
Frumau, K.F., Burkard, R., Schmid, S., Bruijnzeel, L.A., Tobón, C., Calvo-Alvarado, J.C., 2011. A comparison of the performance of three types of passive fog gauges under conditions of wind-driven fog and precipitation. Hydrol. Process. 25 (3), 374–383.
Garcia-Estringana, P., Alonso-Blázquez, N., Alegre, J., 2010. Water storage capacity, stemflow and water funneling in Mediterranean shrubs. J. Hydrol. 389 (3), 363–372.
Gash, J.H.C., 1979. An analytical model of rainfall interception by forests. Q. J. Roy. Meteor. Soc. 105 (443), 43–55.
Gash, J.H.C., Wright, I.R., Lloyd, C.R., 1980. Comparative estimates of interception loss from three coniferous forests in Great Britain. J. Hydrol. 48 (1–2), 89–105.
Gash, J.H.C., Lloyd, C.R., Lachaud, G., 1995. Estimating sparse forest rainfall interception with an analytical model. J. Hydrol. 170, 79–86.
Gentry, A.H., 1988. Changes in plant community diversity and floristic composition on environmental and geographical gradients. Ann. Mo. Bot. Gard. 1–34.
Giambelluca, T.W., DeLay, J.K., Nullet, M.A., Scholl, M.A., Gingerich, S.B., 2011. Canopy water balance of windward and leeward Hawaiian cloud forests on Haleakalā, Maui, Hawai'i. Hydrol. Process. 25 (3), 438–447.
Goldsmith, G.R., Matzke, N.J., Dawson, T.E., 2013. The incidence and implications of clouds for cloud forest plant water relations. Ecol. Lett. 16 (3), 307–314.
Gómez-Peralta, D., Oberbauer, S.F., McClain, M.E., Philippi, T.E., 2008. Rainfall and cloud-water interception in tropical montane forests in the eastern Andes of Central Peru. For. Ecol. Manag. 255 (3), 1315–1325.
González-Martínez, T.M., Williams-Linera, G., Holwerda, F., 2017. Understory and small trees contribute importantly to stemflow of a lower montane cloud forest. Hydrol. Process 31, 1174–1183.
Grubb, P.J., 1977. Control of forest growth and distribution on wet tropical mountains: with special reference to mineral nutrition. Annu. Rev Ecol Syst. 8 (1), 107.
Guillod, B.P., Orlowsky, B., Miralles, D., Teuling, A.J., Blanken, P.D., Buchmann, N., Ciais, P., Ek, M., Findell, K.L., Gentine, P., Lintner, B.R., 2014. Land-surface controls on afternoon precipitation diagnosed from observational data: uncertainties and confounding factors. Atmos. Chem. Phys. 14 (16), 8343–8367.
Gupta, H.V., Kling, H., Yilmaz, K.K., Martinez, G.F., 2009. Decomposition of the mean squared error and NSE performance criteria: implications for improving hydrological modelling. J. Hydrol. 377 (1-2), 80–91.
Hafkenscheid, R.L., 2000. Hydrology and Biogeochemistry of Tropical Montane Rain Forests of Contrasting Stature in the Blue Mountains, Jamaica. Vrije Universiteit, Amsterdam, The Netherlands pp. 302, PhD Thesis.
Herwitz, S.R., 1985. Interception storage capacities of tropical rainforest canopy trees. J. Hydrol. 77, 237–252.
Hidalgo, H.G., Cayan, D.R., Dettinger, M.D., 2005. Sources of variability of evapotranspiration in California. J. Hydrometeor. 6, 3–19.
Holder, C.D., Gibbes, C., 2017. Influence of leaf and canopy characteristics on rainfall interception and urban hydrology. Hydrolog. Sci. J. 62 (2), 182–190.
Hölscher, D., Köhler, L., van Dijk, A.I., Bruijnzeel, L.S., 2004. The importance of epiphytes to total rainfall interception by a tropical montane rain forest in Costa Rica. J. Hydrol. 292 (1), 308–322.
Hölscher, D., Köhler, L., Kappelle, M., Leuschner, C.H., 2011. Ecology and use of old-growth and recovering montane oak forests in the Corsillera de Talamanca, Costa Rica. In: Bruijnzeel, L.A., Scatena, F.N., Hamilton, L.S. (Eds.), Tropical Montane Cloud Forests. Cambridge University Press, Cambridge, pp. 610–617.
Holwerda, F., Bruijnzeel, L.A., Muñoz-Villers, L.E., Equihua, M., Asbjornsen, H., 2010. Rainfall and cloud water interception in mature and secondary lower montane cloud forests of central Veracruz. Mexico. J. Hydrol. 384 (1), 84–96.
Holwerda, F., Alvarado-Barrientos, M.S., González-Martínez, T.M., 2016. Surface energy

exchange in a tropical montane cloud forest environment: flux partitioning, and seasonal and land cover-related variations. Agr. For. Meteorol. 228, 13–28.
Hooke, R.L., Martín-Duque, J.F., Pedraza, J., 2012. Land transformation by humans: a review. GSA Today 22 (12), 4–10.
Jackson, L.J., 1975. Relationships between rainfall parameters and interception by tropical forest. J. Hydrol. 24, 215–238.
Jiménez-Muñoz, J.C., Mattar, C., Barichivich, J., Santamaría-Artigas, A., Takahashi, K., Malhi, Y., Sobrino, J.A., Van Der Schrier, G., 2016. Record-breaking warming and extreme drought in the Amazon rainforest during the course of El Niño 2015–2016. Sci. Rep. 6.
Juvik, J.O., Nullet, D., 1995. Comments on "A proposed standard fog collector for use in high-elevation regions.". J. Appl. Meteorol. 34, 2108–2110.
Klaassen, W., 2001. Evaporation from rain-wetted forest in relation to canopy wetness, canopy cover, and net radiation. Water Resour. Res. 37 (12), 3227–3236.
Lawton, R.O., Putz, F.E., 1988. Natural disturbance and gap-phase regeneration in a wind-exposed tropical cloud forest. Ecology 69 (3), 764–777.
Lawton, R.O., Nair, U.S., Pielke, R.A., Welch, R.M., 2001. Climatic impact of tropical lowland deforestation on nearby montane cloud forests. Science 294 (5542), 584–587.
Letts, M.G., Mulligan, M., 2005. The impact of light quality and leaf wetness on photosynthesis in north-west Andean tropical montane cloud forest. J. Trop. Ecol. 21, 549–557.
Levenberg, K., 1944. A method for the solution of certain non-linear problems in least squares. Q. Appl. Math. 2 (2), 164–168.
Magrin, G.O., Marengo, J.A., Boulanger, J.-P., Buckeridge, M.S., Castellanos, E., Poveda, G., Scarano, F.R., Vicuña, S., 2014. Central and South America. In: Barros, V.R., Field, C.B., Dokken, D.J., Mastrandrea, M.D., Mach, K.J., Bilir, T.E., Chatterjee, M., Ebi, K.L., Estrada, Y.O., Genova, R.C., Girma, B., Kissel, E.S., Levy, A.N., MacCracken, S., Mastrandrea, P.R., White, L.L. (Eds.), Climate Change 2014: Impacts, Adaptation, and Vulnerability. Part B: Regional Aspects. Contribution of Working Group II to the Fifth Assessment Report of the Intergovernmental Panel of Climate Change. Cambridge University Press, Cambridge, United Kingdom and New York, NY, USA, pp. 1499–1566.
Marquardt, D.W., 1963. An algorithm for least-squares estimation of nonlinear parameters. SIAM J. Appl. Math. 11 (2), 431–441.
Marzol, M.V., 2008. Temporal characteristics and fog water collection during summer in Tenerife (Canary Islands, Spain). Atmos. Res. 87 (3-4), 352–361.
McGill, R., Tukey, J.W., Larsen, W.A., 1978. Variations of box plots. Am. Stat. 32 (1), 12–16.
Melsen, L.A., Teuling, A.J., Berkum, S.W., Torfs, P.J.J.F., Uijlenhoet, R., 2014. Catchments as simple dynamical systems: a case study on methods and data requirements for parameter identification. Water Resour. Res. 50 (7), 5577–5596.
Monteith, J.L., 1965. Evaporation and environment. In: the State and movement of water in living organisms. Proceedings of the 19th Symposium Soc. Exp. Biol., Swansea 1964. Academic Press, for the Society for Experimental Biology, UK, pp. 205–234.
Mulligan, M., 2011. Modeling the tropics-wide extent and distribution of cloud forest and cloud forest loss, with implications for conservation priority. In: Bruijnzeel, L.A., Scatena, F.N., Hamilton, L.S. (Eds.), Tropical Montane Cloud Forests. Cambridge University Press, Cambridge, pp. 14–38.
Mulligan, M., Jarvis, A., González, J., Bruijnzeel, L.A., 2011. Using "biosensors" to elucidate rates and mechanisms of cloud water interception by epiphytes, leaves, and branches in a sheltered Colombian cloud forest. In: Bruijnzeel, L.A., Scatena, F.N., Hamilton, L.S. (Eds.), Tropical Montane Cloud Forests. Cambridge University Press, Cambridge, pp. 249–260.
Muñoz-Villers, L.E., Holwerda, F., Gómez-Cárdenas, M., Equihua, M., Asbjornsen, H., Bruijnzeel, L.A., Marín-Castro, B.E., Tobón, C., 2012. Water balances of old-growth and regenerating montane cloud forests in central Veracruz. Mexico. J. Hydrol. 462, 53–66.
Muzylo, A., Llorens, P., Valente, F., Keizer, J.J., Domingo, F., Gash, J.H.C., 2009. A review of rainfall interception modelling. J. Hydrol. 370 (1), 191–206.
Nash, J.E., Sutcliffe, J.V., 1970. River flow forecasting through conceptual models part I-A discussion of principles. J. Hydrol. 10 (3), 282–290.
Oliveira, R.S., Eller, C.B., Bittencourt, P.R.L., Mulligan, M., 2014. The hydroclimatic and ecophysiological basis of cloud forest distributions under current and projected climates. Ann. Bot. 113, 909–920.
Pappenberger, F., Beven, K.J., 2004. Functional classification and evaluation of hydrographs based on multicomponent mapping (Mx). Int. J.River Basin Manag. 2 (2), 89–100.
Piao, S., Friedlingstein, P., Ciais, P., de Noblet-Ducoudré, N., Labat, D., Zaehle, S., 2007. Changes in climate and land use have a larger direct impact than rising CO2 on global river runoff trends. Proc. Natl. Acad. Sci. 104 (39), 15242–15247.
Ponette-González, A.G., Weathers, K.C., Curran, L.M., 2010. Water inputs across a tropical montane landscape in Veracruz, Mexico: synergistic effects of land cover, rain and fog seasonality, and interannual precipitation variability. Glob. Chang. Biol. 16 (3), 946–963.
Prada, C.M., Stevenson, P.R., 2016. Plant composition associated with environmental gradients in tropical montane forests (Cueva de los Guacharos National Park, Huila, Colombia). Biotropica 48 (5), 568–576.
Pryet, A., Dominguez, C., Tomai, P.F., Chaumont, C., d'Ozouville, N., Villacís, M., Violette, S., 2012. Quantification of cloud water interception along the windward slope of Santa Cruz Island, Galapagos (Ecuador). Agr. For. Meteorol. 161, 94–106.
Ramírez, B.H., Teuling, A.J., Ganzeveld, L., Hegger, Z., Leemans, R., 2017a. Tropical Montane Cloud Forests: hydrometeorological variability in three neighbouring catchments with different forest cover. J. Hydrol. 552, 151–167.
Ramírez, B., van der Ploeg, M., Teuling, A.J., Ganzeveld, L., Leemans, R., 2017b. Tropical Montane Cloud Forests in the Orinoco River Basin: the role of soil organic layers in water storage and release. Geoderma 298, 14–26.
Ray, D.K., Nair, U.S., Lawton, R.O., Welch, R.M., Pielke, R.A., 2006. Impact of land use on Costa Rican tropical montane cloud forests: sensitivity of orographic cloud formation to deforestation in the plains. J. Geophys. Res. 111, D02108. http://dx.doi.org/10.1029/2005JD006096.
Reinhardt, K., Smith, W.K., 2008. Impacts of cloud immersion on microclimate, photosynthesis and water relations of Abies fraseri (Pursh.) Poiret in a temperate mountain cloud forest. Oecologia 158, 229–238. http://dx.doi.org/10.1007/s00442-008-1128-5.
Roa-García, M.C., Brown, S., Schreier, H., Lavkulich, L.M., 2011. The role of land use and soils in regulating water flow in small headwater catchments of the Andes. Water Resour. Res. 47, W05510.
Rutter, A.J., Morton, A.J., 1977. A predictive model of rainfall interception in forests. III. Sensitivity of the model to stand parameters and meteorological variables. J. Appl. Ecol. 567–588.
Rutter, A.J., Kershaw, K.A., Robins, P.C., Morton, A.J., 1971. A predictive model of rainfall interception in forests, 1. Derivation of the model from observations in a plantation of Corsican pine. Agr. Meteorol. 9, 367–384.
Rutter, A.J., Morton, A.J., Robins, P.C., 1975. A predictive model of rainfall interception in forests. II. Generalization of the model and comparison with observations in some coniferous and hardwood stands. J. Appl. Ecol. 367–380.
Scatena, F., Bruijnzeel, L., Bubb, P., Das, S., et al., 2011. Setting the stage. In: Bruijnzeel, L.A. (Ed.), Tropical Montane Cloud Forests. International Hydrology Series. Cambridge University Press, Cambridge, pp. 3–13.
Schellekens, J., Scatena, F.N., Bruijnzeel, L.A., Wickel, A.J., 1999. Modelling rainfall interception by a lowland tropical rain forest in northeastern Puerto Rico. J. Hydrol. 225 (3), 168–184.
Stallard, R., Koehnken, L., Johnsson, M., 1991. Weathering processes and the composition of inorganic material transported through the Orinoco River system, Venezuela Colombia. Geoderma. 51, 133–165. http://dx.doi.org/10.1016/0016-7061(91)90069-6.
Stevenson, P., Casas, L., 2008. Plantas del norte del municipio de Chámeza. In: Ramírez, B. (Ed.), Informe Técnico "Levantamiento y análisis de información necesaria para la elaboración del plan de acción que permita obtener la declaratoria de área protegida del bosque ubicado al norte del municipio de Chámeza". Asociación de Becarios de Casanare y Municipio de Chámeza, pp. 31–36.
Still, C., Foster, P., Schneider, S., 1999. Simulating the effects of climate change on tropical montane cloud forests. Nature 398, 15–17.
Tanaka, N., Kuraji, K., Tantasirin, C., Takizawa, H., Tangtham, N., Suzuki, M., 2011. Relationships between rainfall, fog and throughfall at a hill evergreen forest site in northern Thailand. Hydrol. Process. 25 (3), 384–391.
Thornton, P.E., Running, S.W., 1999. An improved algorithm for estimating incident daily solar radiation from measurements of temperature, humidity, and precipitation. Agric. For. Meteorol. 93, 211–228. http://dx.doi.org/10.1016/S0168-1923(98)00126-9.
Tobón, C., Köhler, L., Frumau, K.F.A., Bruijnzeel, L.A., Burkard, R., Schmid, S., 2010. Water dynamics of epiphytic vegetation in a lower montane cloud forest: fog interception, storage and evaporation. In: Bruijnzeel, L.A., Scatena, F.N., Hamilton, L.S. (Eds.), Tropical Montane Cloud Forests. Cambridge University Press, Cambridge, pp. 261–267.
Van Dijk, A.I.J.M., Peña-Arancibia, J.L., 2012. Land cover and water yield: inference problems when comparing catchments with mixed land cover. Hydrol. Earth Syst. Sc. 16 (9), 3461–3473.
Villegas, J.C., Tobón, C., Breshears, D.D., 2008. Fog interception by non-vascular epiphytes in tropical montane cloud forests: dependencies on gauge type and meteorological conditions. Hydrol. Process. 22 (14), 2484–2492.
Vrugt, J.A., Dekker, S.C., Bouten, W., 2003. Identification of rainfall interception model parameters from measurements of through-fall and forest canopy storage. Water Resour. Res. 39 (9).
Wagener, T., Sivapalan, M., Troch, P.A., McGlynn, B.L., Harman, C.J., Gupta, H.V., Kumar, P., Rao, P.S.C., Basu, N.B., Wilson, J.S., 2010. The future of hydrology: an evolving science for a changing world. Water Resour. Res. 46, W05301.
Wallace, J., McJannet, D., 2012. Climate change impacts on the water balance of coastal and montane rainforests in northern Queensland, Australia. J. Hydrol. 475, 84–96.
Wallace, J., McJannet, D., 2013. How might Australian rainforest cloud interception respond to climate change? J. Hhydrol. 481, 85–95.
Weiss, M., Baret, F., 2014. CAN-EYE User Manual.
Wullaert, H., Pohlert, T., Boy, J., Valarezo, C., Wilcke, W., 2009. Spatial through-fall heterogeneity in a montane rain forest in Ecuador: extent, temporal stability and drivers. J. Hydrol. 377 (1), 71–79.
Zadroga, F., 1981. The hydrological importance of a montane cloud forest area of Costa Rica. In: Lal, R., Russell, E.W. (Eds.), Tropical Agricultural Hydrology. John Wiley and Sons, New York, pp. 59–73.